ARTICLE

Sympatric and allopatric evolutionary contexts shape differential immune response in *Biomphalaria / Schistosoma* interaction.

Anaïs Portet[1], Silvain Pinaud[1,#], Cristian Chaparro[1], Richard Galinier[1], Guillaume M. Charriere[2], Jean-François Allienne[1], David Duval[1], Benjamin Gourbal[1§]

[1] Univ. Perpignan Via Domitia, Interactions Hôtes Pathogènes Environnements UMR 5244, CNRS, IFREMER, Univ. Montpellier, F-66860 Perpignan, France

[2] Interactions Hôtes-Pathogènes-Environnements (IHPE), UMR 5244, CNRS, Ifremer, Université de Perpignan Via Domitia, Université de Montpellier, Montpellier, 34095, France.

present address : Wellcome Trust Sanger Institute, Hinxton, CB10 1SA, UK

[§] corresponding author:

Benjamin Gourbal

UMR5244 IHPE, Université de Perpignan

58 avenue Paul Alduy, 66860 Perpignan

benjamin.gourbal@univ-perp.fr

Abstract

Selective pressures between hosts and their parasites can result in reciprocal evolution or adaptation of specific life history traits. Local adaptation of resident hosts and parasites should lead to host-parasite systems performing better in sympatry when compared to allopatry. Between-population variations in parasite infectivity/virulence and host defence/resistance, referred to as compatibility phenotype, were often the proxy used to analyse sympatric or allopatric adaptation. Nevertheless, some reported cases exist where allopatric host-parasite systems demonstrate compatibility phenotypes similar or greater than the one observed in sympatry. In these cases, the role of local adaptation is worth considering. Here, we study the interaction between *Schistosoma* and its vector snail *Biomphalaria* in which such a discrepancy in local versus foreign compatibility phenotype has been observed. Herein, we developed an integrative approach to investigate sympatric and allopatric interaction processes and link the underlying molecular mechanisms to the resulting phenotypes. Using comparative "omics" approaches joined to analysis of life history traits (immune cellular response, mortality, prevalence and compatibility) we tried to bridge the gap of knowledge that exists for connecting local adaptation observations to molecular phenotypes in *Schistosoma/Biomphalaria* interactions.

We found that despite displaying similar prevalence phenotypes, parasite infection triggered an immune suppression in snails living in sympatry, while it activated an immune response for those living in allopatry. Dual-comparative molecular analyses revealed that parasite infection causes immune suppression in sympatry. miRNAs were used to hijack the host's immune response, allowing sympatric parasites to initiate their developmental program earlier and more efficiently.

We show that despite having similar prevalence phenotypes, sympatric and allopatric snail-*Schistosoma* interactions displayed a strongly different immunobiological molecular dialogue. The ability of allopatric pathogens to adapt rapidly and efficiently to new hosts could have critical consequences on disease emergence and risk of schistosomiasis outbreaks. These observations would have important consequences in term of schistosomiasis disease control.

Keywords: sympatry, allopatry, host-parasite compatibility, RNA-seq, immunity

Introduction

Schistosomiasis is the second most widespread human parasitic disease after malaria and affects more than 200 million people worldwide (1). *Schistosoma mansoni* (Platyhelminthes, Lophotrochozoa) causes intestinal schistosomiasis. *Schistosoma* needs a mollusc (belonging to *Biomphalaria, Bulinus* or *Planorbarius* genus) to act as its first intermediate host, where it undergoes part of its life cycle before infecting humans. Patently infected snails support the continuous production of thousands of cercariae, the free-living human-infective stage of the parasite, until dying. As such, vector snails appear to be a central actor in the parasite transmission and thus have deserved greater attention as a potential target for schistosomiasis control. To achieve this objective, it is necessary to understand snail-parasite immunobiological interactions and characterize the molecular mechanisms by which snails and *Schistosoma* interact.

Biomphalaria/Schistosoma compatibility is based on a complex phenotype-to-phenotype or matching-phenotype model (2-7). The success or failure of the infection of *B. glabrata* by *S. mansoni* reflects a complex interplay between the host's defence mechanisms and the parasite's infective strategies. In the past 15 years, the molecular basis of this compatibility polymorphism has been investigated at the genomic level (8-10), the transcriptomic level (6, 11-15), the proteomic level (16-23) and the epigenomic level (24-29). These studies have revealed that various molecules and pathways involved in immune recognition (snail immune receptors versus parasite antigens), immune effector/anti-effector systems and immune regulation/activation participate in a complex interplay that governs the match or mismatch of host and parasite phenotypes (30). This complex phenotype-by-phenotype interaction (compatibility polymorphism) varies between populations and individuals resulting in "multi-parasite susceptibility" or "multi-host infectivity" phenotypes (5) that reflect between-population variations in parasite infectivity/virulence and host defence/resistance (31, 32).

In *B. glabrata/Schistosoma sp.* models, numerous sympatric and allopatric combinations have been tested: (i) different *B. glabrata* laboratory strains (or isolates) show various degrees of susceptibility to *S. mansoni* infection, and (ii) different strains of *S. mansoni* display different levels of infectivity toward a particular strain of snail host (2, 4, 5, 33, 34). In most cases, interaction in *B.*

glabrata/Schistosoma models has been investigated by comparing, (i) sympatric/compatible and (ii) allopatric/incompatible host-parasite associations. Indeed, the general assumption is that the parasites, which have a shorter generation time, larger population sizes and higher reproductive outputs, are ahead in the co-evolutionary conflict against their host and are therefore more likely to locally adapt to them (35, 36). This is exactly what is stated by the "host-parasite local adaptation hypothesis", in which the sympatric parasite is supposed to perform better than the allopatric one (36-39). However, it has been observed that compatibility phenotypes between *Biomphalaria* and *Schistosoma* were the same comparing sympatric and allopatric combinations or even greater for allopatric parasites, and thus did not fulfil the "local versus foreign" criterion of the "host-parasite local adaptation hypothesis" (33, 40, 41). Such compatibility phenotypes have been mostly investigated in terms of parasite infectivity or pathogenicity toward snail hosts, but to our knowledge very few studies have investigated the molecular basis of allopatric compatible interactions from the perspective of both sides of the interaction, the host and parasite (42, 43).

Hence, in order to bridge this gap, we herein study sympatric/allopatric interactions displaying similar compatibilities using an integrative approach that links the underlying molecular mechanisms to the resulting phenotypes, based on comparative molecular approaches on both host snails and *Schistosoma* parasites. We set out to analyse the compatibility between South American snail strains (from Recife Brazil and Guacara Venezuela) in combination with three different parasite isolates that displayed nearly the same compatibility phenotype: (i) *S. mansoni* Recife Brazil, (ii) *S. mansoni* Guacara Venezuela (both sympatric and allopatric, narrow geographic scale) and (iii) *S. rodhaini* from Burundi Africa (allopatric, large geographic and phylogenetic scales). Thus, even if compatibility phenotypes (prevalence/intensity) are similar, the characterization of the underlying molecular mechanisms demonstrates a very different immunobiological dialogue between *B. glabrata* vector snails and their sympatric or allopatric *Schistosoma* parasites at the cellular and molecular scales.

To the best of our knowledge very few studies have investigated the molecular basis of local adaptation in host/parasite interactions (44, 45). Here we used a powerful global approach to identify the differentially regulated transcripts in snails of a single *B. glabrata* strain under infection by three sympatric or allopatric compatible strains or species of the parasite, *Schistosoma sp.*

Moreover, our results may be of critical importance in terms of schistosomiasis control. Understanding the mechanisms whereby allopatric parasites efficiently infect host snails, would be essential to develop new tools to predict or quantify risks of schistosomiasis disease outbreaks (46).

Materials and Methods

Ethical statements

Our laboratory holds permit # A66040 for experiments on animals, which was obtained from the French Ministry of Agriculture and Fisheries and the French Ministry of National Education, Research, and Technology. The housing, breeding and care of the utilized animals followed the ethical requirements of our country. The experimenter possesses an official certificate for animal experimentation from both of the above-listed French ministries (Decree # 87–848, October 19, 1987). The various protocols used in this study have been approved by the French veterinary agency of the DRAAF Languedoc-Roussillon (Direction Régionale de l'Alimentation, de l'Agriculture et de la Forêt), Montpellier, France (authorization # 007083).

Biological materials

Two snail strains of *Biomphalaria glabrata* were used in this study: the albino Brazilian strain, (BgBRE) and the Venezuelan strain, (BgVEN). They were exposed to infection by a Brazilian (SmBRE) or Venezuelan (SmVEN) strain of *Schistosoma mansoni*, or by another *Schistosoma* species, *S. rodhaini* (Srod). All host and parasite strains of each different geographical origin were recovered in their native locality and maintained in the laboratory always on their sympatric snail hosts to maintain reciprocal selective pressures and reciprocal sympatric strain adaptation. We housed snails in tanks filled with pond water at 25°C with a 12:12 hour light:dark cycle and supplied *ad libitum* with fresh lettuce. The Brazilian strain originates from the locality of Recife (east Brazil), the Venezuelan strains of snail and parasite were recovered from the locality of Guacara (north Venezuela) and the African species *Schistosoma rodhaini* originates from Burundi and was obtained from the London British Museum. These *Schistosoma* isolates/species have been selected because they exhibited similar infectivity toward BgBRE or BgVEN strains (see prevalence and intensity in

136 supplementary table S1). Prevalence of SmBRE and SmVEN for the African vector snail
137 *Biomphalaria pfeifferi* from Senegal (BpSEN), and prevalence of the corresponding parasite SmSEN
138 on South American snails were also tested (supplementary table S1).
139
140 *RNAseq experimental protocol*
141 In order to investigate the molecular response of snails against sympatric and allopatric parasites, a
142 global comparative transcriptomic approach was conducted. One hundred and twenty BgBRE snails
143 were infected with SmBRE, SmVEN or Srod. Each snail was individually exposed for 12 h to 10
144 miracidia in 5mL of pond water. For each experimental infection, 20 snails were recovered at 24 and
145 96 h after infection. The samples were named as follows: BB24, BB96 for BgBRE infected with
146 SmBRE; BV24, BV96 for BgBRE infected with SmVEN; and BR24, BR96 for BgBRE infected with
147 Srod. Two pools of 30 uninfected BgBRE snails (Bre1 and Bre2) were used as controls.
148 - Whole-snail RNA extraction and sequencing
149 Total RNA was extracted using TRIZOL® (Sigma Life Science, USA) according to the
150 manufacturer's instructions. Sequencing was performed using paired-end 72-bp read lengths on
151 Illumina Genome Analyzer II (MGX-Montpellier GenomiX, Montpellier, France).
152 - De novo transcriptome assembly
153 *De novo* transcriptome assembly, using all time points, was performed using an in-house pipeline
154 created with the Velvet (1.2.02), Oases (v0.2.04) and CD-HIT-EST (v4.5.4) programs. The assembly
155 of the consensus reference transcriptome was optimized using various parameters, including k-mer
156 length, insert length and expected coverage, as previously described (47, 48). A de novo transcriptome
157 was created that contained 159,711 transcripts.
158 - Differential expression analysis
159 High-quality reads (Phred score >29) were aligned to the de novo transcriptome using Bowtie2
160 (v2.0.2), which was run locally on a Galaxy server. To compare the host responses during the
161 sympatric or allopatric interactions, we used the DESeq2 (v2.12) software to analyse the differential
162 transcript representation between *BgBRE* control strains (uninfected *Bg*BRE1 and *Bg*BRE2) to the
163 sympatric and allopatric conditions (p-value < 0.1) (48). A Venn diagram was generated using the

164 Venny 2.1 software to highlight which differentially expressed transcripts were specific or common to
165 the different interactions. A heatmap was then created to analyse transcript expression patterns, using
166 log2 Fold Change with Hierarchical Ascending Clustering (HAC) and Pearson correlation
167 (uncentered) as applied by the Cluster (v3.0) and Java TreeView (v1.1.6r4) software packages. The
168 differentially represented transcripts were functionally classified using a BlastX analysis with the cut-
169 off set to e-value < $1e^{-3}$ (NCBI dataset; thanks to the Roscoff Data center Cluster, UPMC) and gene
170 ontology was assigned using an automatic annotation, Blast2GO (v3.0.8) (supplementary table S2).
171 Based on automatic annotation and functional domains and according to the literature we identified the
172 potential immune transcripts involved in snail immunity.
173
174 *Schistosoma intra-molluscal stage transcriptome analysis: Dual RNA-seq*
175 Host response against pathogens constitutes solely one side of the molecular dialogue occurring in
176 host/parasite interactions. To analyse all the complexity of such dialogue, the parasite response into
177 host tissue also needs to be investigated. Herein a dual RNA-seq approach was thus conducted to gain
178 a broader understanding of sympatric and allopatric host/parasite interactions.
179 - Schistosome read selection
180 The *Biomphalaria* (v1) and *Schistosoma* (v5.2) genomes have been concatenated
181 (https://www.vectorbase.org/organisms/biomphalaria-glabrata;
182 http://www.sanger.ac.uk/resources/downloads/helminths/schistosoma-mansoni.html). High-quality
183 reads (Phred score > 29) were mapped against these concatenated genomes using Bowtie2 (v2.0.2),
184 which was run locally on the Galaxy project server. The reads that mapped only once and exclusively
185 to the *Schistosoma* genome were collected as corresponding to *Schistosoma* reads; reads that mapped
186 to the *Biomphalaria* genome or more than once to either genomes were removed from the analysis.
187 - Gene analysis
188 The above-selected *Schistosoma* reads were mapped against the concatenate genome to identify intra-
189 molluscal stage-specific *Schistosoma* genes. In order to select the relevant genes, the reads mapped in
190 all experimental conditions were summed. Only genes with a minimal sum of 10 reads were kept for
191 the analysis. A heatmap was generated to analyse *Schistosoma* gene expression patterns using

192 Hierarchical Ascending Clustering (HAC) with Pearson correlation (uncentered) as applied by the
193 Cluster (v3.0) and Java TreeView (v1.1.6r4) software packages. Functional annotation of the genes
194 was assigned using BlastX with the cut-off set to e-value < $1e^{-3}$ (NCBI dataset, local cluster) and gene
195 ontology was performed using Blast2GO (v4.0.7) (supplementary table S3).
196
197 *Innate immune cellular response analysis: microscopy and flow cytometry*
198 Hemocytes appeared as the main cells supporting the *Biomphalaria* snail immune response. Thus, to
199 go further in the description of snail response against parasites, quantitative and qualitative changes in
200 hemocyte populations were investigated. For this purpose, BgBRE and BgVEN snails were used.
201 Snails were infected as described above, using either SmBRE or SmVEN parasites. For each
202 experimental infection, snails were recovered at 24 and 96 h after infection and designated as follows:
203 BB24 and BB96 for BgBRE infected with SmBRE; BV24 and BV96 for BgBRE infected with
204 SmVEN; VV24 and VV96 for BgVEN infected with SmVEN; and VB24 and VB96 for BgVEN
205 infected with SmBRE. Snails of each strain, BgBRE and BgVEN, were recovered and used as
206 controls.
207 - Hemocyte proliferation analysis: microscopy
208 Microscopic inspection of hemocyte proliferation was conducted using 12 infected BgBRE (6
209 BgBRExSmBRE and 6 BgBRExSmVEN) and 3 uninfected BgBRE snails. The hemocytes of 3 snails
210 (biological replicates) were counted for each condition at 24 h and 96 h after infection. The
211 proliferation of circulating hemocytes was studied by using a Click-iT EdU Alexa Fluor 488 Flow
212 Imaging Kit (Molecular Probes). At each time point, circulating hemocytes were recovered by direct
213 puncture after foot retraction and 1mM of EdU solution was added to the hemolymph. Three hours
214 later, the amount of EdU incorporated by the circulating hemocytes was visualized in vitro after
215 fixation of the cells and performing a covalent coupling of Alexa Fluor 488 to the EdU residues trough
216 a click chemistry reaction flowing manufacturer indications. Next, nuclei of hemocytes were
217 counterstained with DAPI (Biotum) staining, and the sample was analysed on a confocal microscope
218 using a Zeiss LSM 700, with 4 lasers (405, 488, 555 and 633 nm). Positive cells were counted and

219 between-sample differences in the percentage of proliferation were tested using a Fisher exact test,
220 with significance accepted at p-value < 0.05.

221 - Hemocyte proliferation and population profiles analysis: flow cytometry

222 Qualitative changes in hemocyte populations following infection by sympatric or allopatric parasites
223 were studied using a flow cytometry approach. For this, 72 infected BgBRE or BgVEN (36 infected
224 by SmBRE and 36 infected by SmVEN) and 18 uninfected BgBRE or BgVEN snails were used. Six
225 biological replicates (pools of three snails per replicate) were performed for each condition. Flow
226 cytometry was used to profile and assess the proliferation of circulating hemocytes using Click-
227 iTEdUAlexa Fluor 647 labelling (Molecular Probes). At each time point, 1mM of EdU solution was
228 injected into pericardial cavity of each snail. Three hours later six replicates of three snails were
229 collected, and the hemolymph was extracted from the head-foot according to standard procedures (49).
230 The hemolymph was pooled from the three snails, and 100 µl were subjected to analysis with the
231 above listed kit, according to the manufacturer's instructions. The percentage of proliferative cells was
232 calculated by flow cytometry.

233 The hemocytes were profiled along the course of infection using Side Scatter Chanel (SSC) to
234 estimate cell granularity and Forward Scatter Chanel (FSC) to estimate cell size. The cell repartition
235 along these two parameters enables the identification of cell subpopulations. The flow cytometry was
236 performed using a FACS Canto from BD Biosciences (RIO Imaging Platform, Montpellier, France).
237 For each sample, 10,000 events were counted. The results were analysed with the FlowJo V 10.0.8
238 software. Between-group differences in the percent of proliferation were tested using the Mann-
239 Whitney U-test, with significance accepted at p-value<0.05.

240

241 *Histological procedures*

242 A histological approach was conducted in order to investigate differences in miracidia to sporocyst
243 development, while comparing sympatric and allopatric parasite growth, development and maturation
244 into snail tissues. BgBRE snails (n=8 per group) were infected as described above with either SmBRE
245 (sympatric) or SmVEN (allopatric) parasites. At 24 and 96 h after infection, two snails were fixed in
246 Halmi's fixative (4.5% mercuric chloride, 0.5% sodium chloride, 2% trichloroacetic acid, 20% formol,

247 4% acetic acid and 10% picric acid-saturated aqueous solution). Both, embedding in paraffin and
248 transverse histological sections (3-μm) were performed using the RHEM platform (Montpellier,
249 France) facilities. The slides were stained using Heidenhain's azan trichromatic staining solution as
250 follows: (i) serial re-hydration was performed in toluene followed by 95%, 70% and 30% ethanol and
251 then distilled water; (ii) coloration was performed using azocarmine G (70% ethanol, 1% aniline, 1%
252 acetic alcohol, distilled water, 5% phosphotungstic acid, distilled water, Heidenhain's azan) and (iii)
253 serial dehydration was performed using 95% ethanol, absolute ethanol, and toluene. The preparations
254 were then mounted with Entellan (Sigma Life Science, St. Louis Missouri, USA) and subjected to
255 microscopic examination. The parasite sizes were measured with the ImageJ software (v2.0.0), and
256 between-group size differences were tested using the Mann-Whitney U-test with statistical
257 significance accepted at a p-value<0.05 based on the mean of the three largest serial cuts of each
258 sporocyst in sympatric or allopatric conditions.
259
260 In-silico *characterization of Schistosoma miRNAs*
261 Parasites may communicate or interfere with their host using different strategies based mainly on
262 excreted/secreted products released into hemolymph. In this context, miRNAs appeared as the most
263 relevant means of communication that can be used by parasites. To test for such a hypothesis *S.*
264 *mansoni* miRNAs were analysed *in-silico* by comparing the relevant miRNA database (miRBase) to
265 our RNAseq libraries generated at the 24 h following sympatric or allopatric infections. S. *mansoni*
266 precursor sequences were downloaded from miRBase (http://www.mirbase.org, 03/09/2017), and
267 high-quality reads from naive (BgBRE) and 24 h post-infection samples (BB24, BV24, BR24) were
268 aligned against a *S. mansoni* sub-database of miRBase, as previously described (50). The identified
269 precursors were confirmed by alignment of high-scoring reads onto precursor and mature miRNAs
270 from miRBase. Only reads with 100% identity were retained for analysis. The localization of each
271 read against miRNA sequence allowed us to identify either the precursor or just the mature miRNA.
272 Precursors found under both naive and infected conditions were excluded to retain exclusively the
273 miRNAs present in samples from infected snails and avoid cross-species contamination because of the
274 potential conserved features of miRNAs from *B. glabrata* and *S. mansoni*.

275 Putative miRNA targets were predicted from among the differentially represented immune-
276 related transcripts (Fig. 1) using Miranda tools (using parameters: Miranda
277 input_miRinput_Transcriptome -out results.txt -quiet -sc 140 -en -15) (51). Because mature miRNAs
278 may exist in two forms depending on which strand (5'-3') of the precursor stem-loop is maturated the
279 predicted interactions could involve the 5' and/or 3' forms, as noted. The results were extracted using
280 the awk tool, listed in supplementary files (Supplementary Table 4), and used to generate a Venn
281 diagram. To confirm the ability of a selected pre-miRNA to produce the stem-loop necessary to
282 produce the mature form, the secondary structures of precursor were predicted using a RNA structure
283 Web tool (http://rna.urmc.rochester.edu/RNAstructureWeb, 03/09/2017) using default parameters.
284
285 *Snail survival analysis*
286 Allopatric or sympatric parasites could have different levels of virulence or impacts on their host that
287 could impair snail survival. To test for such discrepancy we investigated the mortality rates of infected
288 snails over the course of sympatric or allopatric infections. One hundred and sixty BgBRE snails were
289 infected as described above with SmBRE or SmVEN strains (n = 50), and 60 non-infected BgBRE
290 snails were retained as controls. The numbers of dead snails were compiled weekly for 14 weeks. A
291 Kaplan-Meier estimator was used to estimate the survival function from lifetime data. Survival curves
292 were generated using the xlstats Mac software and the log-rank test was applied with significance
293 accepted at $p < 0.05$.
294
295 **Results**
296 *A whole-snail transcriptomic approach for investigating the molecular basis of the innate immune*
297 *response in the sympatric and allopatric contexts*
298 The global transcript representation was analysed using the previously described RNAseq pipeline
299 developed in our laboratory (6, 47, 48). The *Bg*BRE snail host had the same prevalence and intensity
300 phenotypes when exposed to *Sm*BRE, *Sm*VEN or *S*rod parasites (see Supplementary Table 1). Of the
301 159,711 transcripts of the *Bg*BRE transcriptome, 3,865 (2.4%) were differentially represented in all
302 sympatric and allopatric conditions compared to naive snails (Table 1, Supplementary Fig. 1). We

303 performed automatic Blast2GO annotation, discarded the non-annotated transcripts, and retained 1,017
304 annotated transcripts (26.3% of the differentially represented transcripts). Finally, as we were
305 interested in the innate immune response of the snail to the sympatric and allopatric parasites, we
306 focused on transcripts known to have immune-related functions. Of the annotated differentially
307 expressed transcripts, 336 were identified as being immune-related; this subset corresponded to 8.7%
308 of all differentially represented transcripts. The heatmap generated for all differentially represented
309 transcripts is presented in Supplementary Fig. 1.

310 Venn diagrams were used to highlight the relationships of the transcripts that were
311 differentially represented in the *B. glabrata* and *Schistosoma sp.* interactions. Overall, 189, 180 and
312 164 transcripts were differentially represented in the BB (BgBRE/SmBRE, sympatric), BV
313 (BgBRE/SmVEN, allopatric) and BR (BgBRE/Srod, allopatric) interactions, respectively (Fig. 1A).
314 Of the selected transcripts, 40 were shared by the BB, BV and BR interactions (Fig. 1A), and
315 displayed globally the same differentially expressed pattern of expression (Fig. 1B, cluster 1). These
316 transcripts may correspond to the snail's basal immune response against *Schistosoma* parasites.

317 Of the 140 transcripts exclusive to the sympatric (BB) interaction, which represented 74.1% of
318 the immune transcripts found to be differentially represented in this interaction (Fig. 1A), 100% were
319 underrepresented at 24 h post-infection, and 74.6% of these transcripts were observed exclusively at
320 this time point (Fig. 1B, cluster 5).

321 Very similar transcript expression patterns were observed for the two allopatric interactions
322 (BV and BR). Clusters 6 and 7, comprising only 28 and 11 transcripts, were exclusive to BV and BR,
323 respectively. In BV interaction (Fig. 1B, cluster 6), at 96 h after infection 96.5% of the transcripts
324 were expressed: 22% over-represented. In BR interaction (Fig. 1B, cluster 7), 100% of the transcripts
325 were expressed at 96 h after infection: 82% overrepresented. Of the 108 transcripts shared by BV and
326 BR (cluster 3, representing 60% and 65.9 % of the transcripts, respectively) (Fig. 1A; Fig. 1B, cluster
327 3), 98.1% were expressed at 96 h post-infection: 28.2% over-represented (Fig. 1B, cluster 3).

328 Altogether, these results show that the host immune-related transcriptomic response differed
329 widely between the sympatric and allopatric interactions. All of the differentially represented
330 transcripts were under expressed at 24 h after infection in sympatry, while the differentially

331 represented transcripts in allopatry were mostly over expressed at 96 h after infection. Moreover, the
332 sympatric interaction was associated with a strong immunosuppression (Fig. 1B, cluster 5), whereas
333 allopatry yielded an activation of the immune response (Fig. 1B, cluster 3).

334 We decided to explore the function of differentially regulated transcripts between the
335 sympatric and allopatric interactions in order to investigate if these differentially regulated transcripts
336 belong to different functional categories. For that, we performed an automatic annotation with
337 Blast2GO (Supplementary Table 2). Based on automatic annotation and according to the literature we
338 distributed the relevant differentially expressed immune transcripts into three groups: (i) immune
339 recognition molecules, (ii) immune effectors and (iii) immune signalling molecules (Fig. 1C). Then
340 these three groups were subdivided into functional categories (Fig. 2). In the BB sympatric interaction,
341 immune recognition molecules, immune effectors and immune signalling pathways correspond to
342 13.1%, 18.3% and 4.2%, respectively (sums of all relevant transcripts at all infection time points).
343 Among the transcripts distributed into these groups, 89.0% were underrepresented. In the BV
344 allopatric interaction, the three groups corresponded respectively to 10.8%, 12.9% and 8.6% and
345 among them 65.9% were underrepresented. Finally, in the BR allopatric interaction, they
346 corresponded to 12%, 12.5% and 7.8% and 62.5% of them were underrepresented. When we
347 compared the percentage of each immunological group in the sympatric and allopatric interactions, no
348 specific functional subset was particularly repressed in the BB sympatric interaction (Fig. 1C; Fig. 2).
349 In fact, most of the time, the same immune functions were affected in sympatric and allopatric
350 infections but different immune transcripts (grey and black diamond in Fig. 2) showed differential
351 regulation following infections (Fig. 2).

352 The differentially regulated transcripts belonging to the three immunological groups (Fig. 2)
353 were largely involved in immune cellular responses, cell adhesion, extracellular matrix component,
354 cell migration, cell differentiation and cell proliferation. All of these functions were under-represented
355 in sympatric interaction (76%), whereas many were overrepresented in allopatric ones (39%) at 24 h
356 after infections (Fig. 2).

357

358 *Immune cellular responses in the sympatric and allopatric contexts*

359 As the transcriptomic approach indicated that multiple immunobiological functions seem to be altered
360 in the host response during the interaction with the parasites, we next investigated whether differences
361 in immune responses in sympatric versus allopatric infections could be seen at the cellular level.
362 Hemocytes, the snail immune cells, participate directly in the immune response against the parasites,
363 and immune cell activation under an immunological challenge can translate into cell proliferation
364 and/or cell morphology modifications.

365 Thus, to investigate such immune cell activation, cell proliferation was quantified using EdU
366 nuclear labelling (Fig. 3). EdU is a nucleoside analogue of thymine incorporated into DNA during
367 DNA synthesis. This incorporation reflects the mitotic activity of hemocytes. As the two tested
368 allopatric interactions appeared extremely similar at the transcriptomic level, we compared only the
369 BV (allopatric) interaction and BB (sympatric) interaction for further analyses. Circulating hemocytes
370 recovered in snail hemolymph were EdU-labelled in vitro to identify mitotic circulating hemocytes
371 (Fig. 3A). EdU-positive hemocytes were quantified using confocal microscopy and showed that
372 hemocyte proliferation was induced threefold following *Schistosoma* infection in BV compared to BB
373 (Fig. 3B). Twenty-four hours after infection, proliferative circulating cells increase significantly in
374 BV, with 5.2% of proliferative cells compared to BB with 2.6% (Fisher exact test two-tailed $p = 7.6$
375 $e10^{-6}$) (Fig. 3B). Moreover, this result demonstrates for the first time that "circulating" hemocytes are
376 able to proliferate following *Schistosoma* infections.

377 Hemocyte proliferation was assessed using flow cytometry after in vivo EdU-labelling (Fig.
378 4A). At 24 h after infection, the rate of proliferating cells was increased significantly (Mann Whitney
379 U test: $U=36$; $z = -2.8$; $p = 0.0022$) by more than twofold between the allopatric and sympatric
380 interactions, 4.2% compared to 1.8% respectively. At 96 h after infection, there were fewer
381 proliferating cells: the percentage of proliferating hemocytes was similar in sympatric BB interaction
382 compared to the control (1%, Mann Whitney U test: $U = 17$; $z = -0.27$; $p = 0.3936$), while remaining
383 somewhat higher in the allopatric BV interaction (2.3%, Mann Whitney U test: $U = 0$; $z = 2.65$; $p =$
384 0.009).

385 To confirm that our observations were related to the type of interaction rather than to a strain
386 effect, we performed the same experiments using another *Biomphalaria glabrata* strain, BgVEN as the

387 host and SmVEN and SmBRE as the sympatric and the allopatric parasite, respectively (Fig. 4B). The
388 rate of proliferating hemocytes increased significantly (Mann Whitney U test: U = 36; z = -2.8; p =
389 0.0022) by more than threefold between the allopatric (VB: BgVEN/SmBRE) and the sympatric (VV:
390 BgVEN/SmVEN) interactions at 24 h after infection (6.8% compared to 2.0% respectively). At 96 h
391 after infection, both rates were decreased, albeit more for VV (0.1%, Mann Whitney U test: U = 2; z =
392 2.48; p = 0.013) than for VB (2.7%, Mann Whitney U test: U = 36; z = 2.8; p = 0.0022). These results
393 similar to those observed for BgBRE interactions, confirmed that the effects observed at the cellular
394 level were related to the type of interactions (sympatric versus allopatric) rather than to the host or
395 parasite strains used.

396 In addition to the mitotic activity, hemocyte morphology was estimated using flow cytometry
397 by measuring size and granularity. We analysed the circulating hemocyte populations in noninfected
398 versus infected snails in two *B. glabrata* snail strains (BgBRE and BgVEN) in sympatric and
399 allopatric interactions with parasites (Fig. 4C and 4D). Morphology and heterogeneity of circulating
400 hemocytes varied in a similar manner between BgBRE and BgVEN snails subjected to infection (Fig.
401 4C and 4D) and we observed infection-related differences in cell morphology. In noninfected snails,
402 the content of circulating hemocytes was very heterogeneous but appeared to represent a single
403 population that exhibited a continuous gradient of size and granularity (Fig. 4C and 4D), which is
404 typical of *B. glabrata* hemocytes (52). However, hemocyte population heterogeneity changed quickly
405 after infection. In allopatric interactions, 24 h after infection (Fig. 4C, BV24, and 4D, VB24) two
406 populations could be distinguished: a population P1 (corresponding to that seen in noninfected snails)
407 and a population P2 (a new population). P2 cells exhibited increased granularity, retained a high
408 degree of size variability, and showed a mitotic activity, as indicated by EdU labelling (Fig. 4C and
409 4D, red dots). This profile was transitory, with the P2 population disappearing by 96 h after infection
410 (Fig. 4C, BV96, and 4D, VB96). Altogether, these results show that, upon infection, the snail
411 circulating immune cells exhibit a particular population dynamics with transient increase of the mitotic
412 activity associated with morphology modifications that are likely to be involved in the host defence
413 response against the parasite during the interaction. Moreover, this response of the immune cells
414 appears to be exacerbated in the allopatric interaction when compared to the sympatric interaction.

415

416 *Schistosoma growth and development in Biomphalaria tissues*

417 Parasite development

418 To investigate the development of *S. mansoni* in *B. glabrata* tissues, we examined the fate of
419 sporocyst in sympatric and allopatric compatible interactions using a histological approach. For both
420 interactions, miracidia were able to penetrate, transform into primary sporocysts (SpI) and develop. At
421 24 h after infection, we observed a significant difference (Mann Whitney U test: U = 40; z = 4.33; p =
422 1.42 e10^{-6}) in the size of sporocyst from sympatric parasites (11,838 μm^2 average size) versus
423 allopatric parasites (7,402 μm^2 average size) (Fig. 5). This difference was no longer seen 96 h after
424 infection (41,413 μm^2 and 36,920 μm^2, respectively, Mann Whitney U test: U = 280; z = -1.31; p =
425 0.1917) (Fig. 5). These results show that during the early events following infection, the parasites
426 develop more slowly in the allopatric compared to the sympatric interaction; thereafter, however, the
427 allopatric parasites catch up quickly, such that no difference is seen at 96 h post-infection (Fig. 5).

428

429 Parasite transcript expression analysis

430 In order to investigate the biological responses of the parasites within their host, dual RNAseq
431 analyses allowed us to identify regulated transcripts from *Schistosoma* parasites during their intra-
432 molluscal development. The parasite RNAseq data at 24 h after infection revealed five clusters of
433 differentially expressed genes from the sympatric (SmBRE) and the allopatric (SmVEN, Srod)
434 parasite responses (Fig. 6). Cluster 1 corresponds to genes highly expressed and cluster 5 weakly
435 expressed for all parasite strains. Cluster 2 represents genes overexpressed in SmBRE versus SmVEN
436 and Srod. Cluster 3 contained genes overexpressed in SmBRE and SmVEN versus Srod and cluster 4
437 SmBRE and Srod versus SmVEN. In all clusters, the gene expression levels in SmBRE sympatric
438 parasite are always greater than in the other allopatric parasites. Blast2GO annotation helps in
439 characterizing 70% of the 351 genes shown in the five clusters (Supplementary Table 3). According to
440 the global Gene Ontology (GO): 70% of the annotated genes were involved in general metabolism and
441 growth, translation processes, regulation of cellular processes and RNA biosynthesis; 25% were
442 involved in molecular transport or cell organization; and 5% were involved in organism defence or

443 response to stimuli. In all these clusters, we identified six parasite gene products that had been
444 involved in parasite modulation or suppression of snail immunity. These molecules correspond to heat
445 shock proteins (Fig. 6, Clusters 1 and 2) (27); glutathione-S-transferase, NADH dehydrogenase
446 subunit, and calreticulin (Fig. 6, Cluster 2) (20, 53, 54); Alpha-2-macroglobulin (Fig. 6, Cluster 4)
447 (55); von Willebrand factor type EGF with pentraxin domain (Fig. 6, Cluster 5) (56) (see
448 Supplementary Table 3). These particular genes could be involved in the strategy used by the parasite
449 to ensure immunosuppression and favour its development and growth within host tissues.

450 In allopatric interactions, an activation of the immune response is observed. Interestingly,
451 allopatric parasites did not overexpress any transcripts that could have immunosuppressive function or
452 impair the activation of the immune response (Fig. 6 and Supplementary Table 3). Furthermore, a
453 variant of a glycerol-3-phosphate acyl-transferase (Schisto_mansoni.Chr_3.5623) is highly
454 overexpressed in SmVEN and Srod compared to SmBRE (Cluster 1 Supplementary Table 3). This
455 molecule is known to participate in the biosynthesis of phosphatidic acid, itself involved in
456 macrophage activation and regulation of inflammatory signalling (57, 58). This would thus indirectly
457 enhance the cellular immune response of *Biomphalaria glabarata* against those allopatric parasites.

458

459 Parasite microRNAs analysis

460 The microRNAs (miRNAs) are known as noncoding small RNA (<24nt) able to regulate gene
461 expressions. As we identified deep modifications of transcriptional or posttranscriptional activities
462 between sympatric and allopatric interactions, we investigated, in silico, the potential presence of
463 *Schistosoma mansoni* miRNAs in our parasite RNAseq data. At 24 h post infections, we identified 54
464 miRNA precursors from miRBase with high-quality alignment scores against the different RNAseq
465 read libraries (naïve BgBRE, BB24, BV24, BR24). To avoid cross-species misidentifications, we
466 selected precursors that were exclusively identified in infected and never identified in uninfected
467 snails (naive BgBRE). Eleven miRNA precursors corresponding to *Schistosoma mansoni* were
468 identified (Fig. 7A). Eight of the parasite miRNA precursors were specific to the Brazil-infected
469 libraries (BB24); two were specific of the Venezuela-infected libraries (BV24); and one was shared
470 across the three infected conditions (BB24, BV24 and BR24). Although we identified 49 miRNA

471 precursor sequences specific to *S. mansoni* (Fig. 7B), we decided to select only miRNAs covered by
472 100% nucleotide similarity that allowed us to predict 11 miRNAs in mature (e.g., sma-mir-2d-3p,
473 sma-mir-190-3p) or precursor (sma-mir-8431) forms. Then, in order to identify candidate sequences
474 that could represent putative miRNA targets, we used the Miranda tool (Supplementary Table 4). Only
475 RNA-RNA interactions that showed good scores for pairing (> 140) and enthalpy (< 15 Kcal) were
476 considered. The number of targets pertaining to the differentially expressed immune-related transcripts
477 identified in Fig. 1 that were found for the identified miRNAs ranged from two targets for sma-mir-
478 8456,to 50 targets for sma-mir-2d of the differentially expressed immune-related transcripts identified
479 in Fig. 1.

480 The miRNAs identified under the sympatric condition (SmBRE) were predicted to target 43.5%
481 of the differentially represented immune-related transcripts identified in the RNAseq data (Fig. 1B,
482 Fig. 7) whereas 6.8% and 5.1% were targeted in allopatric conditions, SmVEN and Srod, respectively
483 (Fig. 1B, Fig. 7).To explain the similar prevalence between sympatric and allopatric infections we
484 focus our attention on miRNAs that were shared between sympatric and allopatric interactions and we
485 identified one miRNA:sma-miR-190-3p (Fig. 7 and Supplementary Table 4). This miRNA was
486 predicted to bind 17 different targets among which we identified different variants of the fibrinogen-
487 related protein (FREP) family and a cytotoxic/cytolytic humoral factor the biomphalysin. To go
488 further, we look at the expression of those candidates following infection. If FREP transcripts were
489 downregulated in sympatric interactions, it is not always the case in allopatry. However, interestingly
490 all biomphalysin transcripts were underrepresented in sympatric and allopatric interactions.
491 Altogether, these data suggest that the parasites might hijack the host immune response using
492 dedicated miRNAs.

493

494 *Survival of snail following infection*

495 To examine the potential impact of allopatric or sympatric parasites on snail survival, we investigated
496 the mortality rates of infected snails over 4 months. The survival rate was significantly higher for
497 noninfected snails compared to infected snails (sympatric interaction Kaplan-Meier Log Rank test p =
498 1.39 $e10^{-5}$ and allopatric interaction p = 0.0005). However, there was no significant difference in the

499 mortality rates of snails subjected to sympatric versus allopatric interactions: at the end of the
500 experiment, the survival rates were 72% and 65% for the allopatric and sympatric interactions,
501 respectively (Kaplan-Meier Log Rank test p = 0.243) (Supplementary Fig. 2).
502
503 **Discussion**
504 In the natural environment, it is assumed that the parasitic genes responsible for infectivity will evolve
505 alongside the host defence genes, resulting in adaptation of the interactions between local host and
506 parasite populations (59, 60). In this context, local/sympatric parasites were expected to display
507 greater infectiveness, reproductive success and virulence in host populations compared to
508 foreign/allopatric parasites (38, 39, 61, 62). However, in some cases this rule may be contradicted, as
509 certain allopatric parasite-host interactions have been reported to be significantly more compatible
510 than the corresponding sympatric combinations (40, 63). It appears that certain
511 *Biomphalaria/Schistosoma* interactions (64, 65) do not fulfil the "host-parasite local adaptation
512 hypothesis" (38, 39, 61, 62), in which the sympatric parasite is expected to perform better than the
513 allopatric one.
514 Using field data, Morand et al. (1996) and Prugnolle et al. (2006) showed that although sympatric
515 parasite-host combinations of schistosomes and snails do tend to be more compatible, exceptions exist
516 wherein particular allopatric combinations are equally or significantly more compatible. Similar
517 results were obtained when comparing the interactions of Brazilian and Guadeloupean snails versus
518 *Schistosoma* infections (42). The authors found that allopatric Guadeloupean parasites were not able to
519 infect Brazilian snails; but Brazilian parasites were able to infect the allopatric Guadeloupean snails.
520 Furthermore, this work demonstrated the presence of local adaptation between reactive oxygen species
521 (ROS) and ROS scavengers in this system (42). Based on these observations, we propose that it would
522 be important to develop integrative analysis to depict and understand the precise molecular crosstalk
523 (immunobiological interactions) occurring in such highly compatible sympatric and allopatric systems.
524 Thus, dual-comparative approaches were used herein to simultaneously analyse the responses of
525 *Biomphalaria* snails and *Schistosoma* parasites into sympatric or allopatric interactions displaying
526 similar compatibilities.

527 The present RNAseq analysis demonstrated that in sympatric interaction (BB) a huge
528 immunosuppression occurs. Twenty-four hours after the infection, the three immunological processes
529 were downregulated: (i) immune recognition, (ii) effector and (iii) signalling pathways (Fig. 1 and 2).
530 Conversely, in allopatric interactions (BV and BR), host immune response was activated (Fig. 1 and
531 2). Differentially regulated transcripts mostly belong to immune cellular activation, migration,
532 proliferation or differentiation (Fig. 2). An EdU-labelling was used to detect proliferation and to
533 confirm that more hemocyte proliferation was observed in allopatry compared to sympatry (Fig. 3, 4A
534 and 4B). Using flow cytometry, we demonstrated that a new hemocyte subpopulation (named P2) was
535 observed exclusively following allopatric infection at 24 h (Fig. 4C and 4D). P2 was EdU-positive and
536 characterized by an increase in granularity, indicating that the new P2 cell subtype could proliferate.

537 In Biomphalaria snails, we know three main hemocyte morphotypes: the Blast-like cells, the
538 type I hyalinocytes and the granulocytes (66). However, in absence of specific hemocyte markers, it is
539 impossible to analyse which hemocyte morphotypes are proliferating in our flow cytometry results
540 (Figs. 4C, 4D). The P2 subpopulation would thus originate from either a morphological change in an
541 existing subset (correlating potentially with a decline in the P1 population), or represent cells that are
542 migrating from tissues or a hematopoietic organ to reach the hemolymph. Indeed the P2 population
543 reflects newly proliferated cells that present higher EdU positive cells than the P1 population (Fig. 4C,
544 4D). Further investigations will be necessary to determine the origin of the P2 population. However,
545 hemocyte proliferation decreased more rapidly in sympatric versus allopatric interactions (Fig. 3 and
546 4). By comparing different sympatric and allopatric interactions, we demonstrated that the cellular or
547 molecular phenotype observed may refers to reciprocal evolution or adaptation rather to a simple host
548 or parasite strain effect.

549 The strong immunosuppression observed in sympatric interaction compared to the immune
550 cell activation in allopatry certainly results in differences in the capabilities of sympatric and allopatric
551 parasites to infect and grow in such hosts. This hypothesis was confirmed by our histological analysis
552 of sporocyst development in snail tissues. We observed a significant difference in sporocyst size 24 h
553 after infection (Fig. 5), when sympatric sporocysts were one-third bigger than allopatric sporocysts. At
554 96 h after infection, in contrast, there was no size difference between sympatric and allopatric

555 parasites (Fig. 5). This indicates that the allopatric parasites seem to overcome this early delay in
556 development. However, the consequences of this delay for duration of cercariae development, number
557 of cercariae produced, cercariae infectivity and pathogenicity in vertebrate host, will deserves further
558 investigation to determine the potential fitness cost between sympatric and allopatric parasites.

559 To go further and understand how parasites immunosuppress the host or circumvent the host
560 immune system, we used a dual-RNAseq approach to investigate transcripts expression of the
561 sympatric and allopatric parasite intra-molluscal stages (Fig. 6). As the histological differences were
562 solely observed at 24 h after infection, we used dual-RNAseq to investigate the parasite expression
563 patterns at the same time point of infection. Most of the parasite transcripts belonged to the processes
564 of nucleotide metabolism, transcription, translation and cell differentiation, development and growth.
565 We also identified some transcripts with GO terms or functions related to immunomodulation or
566 immunosuppression (Fig. 6 and Supplementary Table 4). Nearly all of the identified transcripts were
567 overrepresented in the sympatric interaction compared to the allopatric interactions. Our results
568 therefore suggest that the installation, development and growth of the parasite occurred much more
569 rapidly in the sympatric combination, as sympatric parasites seemed to interfere more efficiently with
570 the host immune system. However, RNAseq data did not give any clear information about how
571 allopatric parasites succeed in circumventing the host immune system. We thus next examined the
572 generated dual-RNAseq libraries in an effort to identify whether sympatric and/or allopatric
573 schistosomes could hijack the host immune system using microRNAs. To achieve this goal, we
574 confronted the dual-RNAseq data to the *Schistosoma mansoni* subset of miRBase to identify the
575 presence of microRNAs (miRNAs) in our datasets. miRNAs are known to regulate numerous
576 biological processes, including key immune response genes (67, 68). Recent work has demonstrated
577 that circulating small noncoding RNAs from parasites have hijack roles against host metabolism,
578 especially in the interaction of schistosomes with their vertebrate hosts (69-71). Such noncoding
579 RNAs could act as exogenous miRNAs to interfere with or circumvent the host immune system. At 24
580 h after infection, several differentially expressed parasite miRNAs were identified. We investigated
581 the potential role played by these miRNAs on host immune response. We identified some predicted
582 targets of such schistosome miRNAs in the *Biomphalaria* immune reference transcriptome. We found

583 that schistosome miRNAs identified in the snails 24 h after sympatric infection may target 43.5% of
584 the differentially regulated immune transcripts (Fig. 7). In contrast, far fewer correspondences were
585 identified for the allopatric interactions (Fig. 7). The higher proportion of targeted genes in the
586 sympatric interaction may result in the observed efficient immunosuppression, demonstrating a
587 specific co-evolution or adaptation in the transcriptional regulation between sympatric host and
588 parasite. However, even if more host immune genes appeared to be targeted in the sympatric
589 combination compared to the allopatric combination (Fig. 7), both sympatric and allopatric
590 interactions displayed the same phenotype of compatibility. In the allopatric condition, despite the
591 activation of the snail immune response, the parasite is able to develop and succeed to infect the host.
592 This similarity in compatibility phenotype between sympatric and allopatric parasites could potentially
593 results from their ability to target host immune weapons or host genes that regulate the snail innate
594 cellular response. In this context, we were expecting to find miRNAs shared between sympatric and
595 allopatric parasites, that is, miRNAs that tend to weaken the immune system. A unique miRNA was
596 found to be shared by allopatric and sympatric parasites, sma-miR-190-3p, which has been identified
597 and predicted to bind different targets among FREPs and biomphalysin. The FREP family members
598 are known as pathogen recognition receptors (64, 65)). Moreover, FREP knockdown was associated
599 with an increase of snail compatibility toward *Schistosoma* infections (72, 73). Biomphalysin is a key
600 humoral factor involved in cytotoxic/cytolytic activities against *Schistosoma* parasites with the ability
601 to bind miracidia and sporocyst surfaces (17, 74). Moreover, the associated snail transcripts to these
602 molecules are mostly down represented in sympatric and allopatric interactions. The miRNA sma-
603 miR-190-3p is perhaps essential for parasite compatibility. Parasites expressing such miRNA would
604 thus be considered as highly virulent parasites with strong infecting capabilities. By producing
605 dedicated miRNAs, the parasites were potentially able to regulate transcriptional, post-transcriptional,
606 translational and protein stability processes that might help them to subvert the snail's immune
607 defences.

608 Compatibility reflects the outcome of complex immunobiological interactions and depends on:
609 (i) the ability of the snail immune system to recognize and kill the parasite; and (ii) the ability of the
610 parasite to circumvent or evade the host immune response (20, 53, 75). Based on the present

observations, we propose that sympatric and allopatric interactions trigger totally different responses. In the sympatric interaction, the parasite is able to induce a host immunosuppression within the first day of infection, enabling it to infect quickly the host and readily begins its development. In the allopatric interaction, the parasite is not able to neutralize quickly the host immune system, and therefore the parasite is recognized by the host defence system, which mounts a potent immune response. The need for allopatric parasites to resist the immune system seems to disrupt the activation of their developmental program during the first day of infection. However, they seemed to be rapidly able to protect themselves against the host immune response and develop normally in snail tissues 96 h post-infection. Thereafter, in the medium- or long-term, there are no observable differences in the prevalence, intensity or snail survival comparing sympatric and allopatric interactions (Supplementary Table 1, Supplementary Fig. 2).

Thus, we show that despite having similar prevalence phenotypes, sympatric and allopatric snail-*Schistosoma* interactions displayed a very different immunobiological dialogue at the molecular level. Intriguingly, these different immunobiological interactions seem to have no repercussions upon parasite growth at longer term or to host survival. As differences at the molecular level do not correspond apparently to any ecologically meaningful changes in term of fitness, it is not straightforward to demonstrate local adaptation in such systems. However, we do not know if fitness costs could affect other biological traits in sympatric and allopatric interactions, for example, sporocyst II or cercariae production, or cercariae infectivity and pathogenicity towards the vertebrate host. Demonstrating local adaptation would thus appear extremely complex and would indeed deserve further investigation. It is hard to draw the line as to when local adaptation is or is not present. However, our results argue that the differences found at the molecular level may ultimately contribute to the evolution of local adaptation at an ecological level. Nevertheless, the ability for allopatric pathogens to adapt rapidly and efficiently to new hosts could have critical consequences on disease emergence and risk of schistosomiasis outbreaks.

Past events of allopatric parasites reaching new areas of transmission, even in a large geographic scale dispersion, have been largely documented, the most famous example being the schistosomiasis colonization of South America since the slave trade of the 16th through 19th centuries

(76, 77). *Schistosoma* originated in Asia, reached Africa 12 to 19 million years ago (MYA), and gave rise to all *Schistosoma* species known in Africa (77). *S. mansoni* diverged from *S. rodhaini* around 2.8 MYA (76, 78), and thereafter, 400 to 500 years ago, colonized South America (76, 77). This colonization of South America by *S. mansoni* from Africa was rendered possible by the presence of the snail host *Biomphalaria glabrata*. All African species of *Biomphalaria* are monophyletic and seem to have originated from paraphyletic South American clades (79-81). The ancestor of *B. glabrata* appears to have colonized Africa 1 to 5 MYA, giving rise to all 12 species of *Biomphalaria* known today in Africa (82). In South America and the Caribbean islands, *S. mansoni* infects *B. glabrata*; in Africa, it infects mostly *B. pfeifferi* and *B. alexandrina*. We found that South American *S. mansoni* parasites are highly compatible with their sympatric South American snail hosts, whereas African *S. mansoni* parasites display low compatibility phenotype with South American snail hosts (Supplementary Table 1). Interestingly, the South American parasites did not lose their compatibility for African snail hosts; that is, prevalence is similar to African parasites when confronted with African snails (Supplementary Table 1). The recent African origin of South American *Schistosoma* parasites (introduction in South America 400 to 500 years ago) may explain that they have not diverged sufficiently in South America to lose their compatibility for African snail hosts. In this case, the transfer of allopatric parasites from Africa to South American snail hosts have been successful and resulted in the emergence of schistosomiasis in South America.

More recently another case of compatible allopatric parasite emergence have been observed when schistososmiasis reached Europe (83, 84). Here, humans infected in Senegal have imported a hybrid between *Schistosoma haematobium* and *Schistosoma bovis* into Corsica. In this case, urogenital schistosomiasis could be introduced and easily and rapidly spread into this novel area of south Corsica because *Bulinus truncatus* the vector snail of *S. haematobium* was endemic in the Corsica Cavu River (83, 84). However, this allopatric African hybrid parasite was able to adapt efficiently to the new Corsican *B. truncatus* host. If parasite hybridization can potentially have a putative role in increasing the colonization potential of such *S. haematobium*, it would be particularly interesting to analyse and depict the molecular support of such allopatric interactions to predict the potential risk of schistosomiasis outbreaks in other European areas, or other potential transmission foci.

Conclusions

If we hope to draw conclusions regarding the existence of emerging or outbreak risks, we need to develop integrative approaches to explore fine-scale patterns of host-parasite interactions. We must consider the spatial scale at which comparisons are conducted, the patterns of disease occurrence, the population genetics, and the involvement of physiological, immunological and molecular processes. Studying the relevant factors at the relevant timing would be of critical importance in terms of schistosomiasis control. Understanding further, how these allopatric parasites efficiently infect host snails would be mandatory to identify markers and develop new tools to predict or to quantify risks of schistosomiasis outbreaks.

Acknowledgements

We thank Cécile Saint-Béat, Nathalie Arancibia and Anne Rognon for their work and diligence in helping generate some of the data described herein.

Declarations

Ethics approval and consent to participate

Our laboratory holds permit # A66040 for experiments on animals, which was obtained from the French Ministry of Agriculture and Fisheries and the French Ministry of National Education, Research, and Technology. The housing, breeding, and care of the utilized animals followed the ethical requirements of our country. The experimenter possesses an official certificate for animal experimentation from both of the above-listed French ministries (Decree # 87–848, October 19, 1987). The various protocols used in this study have been approved by the French veterinary agency of the DRAAF Languedoc-Roussillon (Direction Régionale de l'Alimentation, de l'Agriculture et de la Forêt), Montpellier, France (authorization # 007083).

Availability of data and material

The datasets generated and/or analysed during the current study are not publicly available due to ongoing analysis of transcriptome but are available from the corresponding author on reasonable request.

Raw read fastq files were submitted to the Sequence Read Archive at NCBI (http://trace.ncbi.nlm.nih.gov/Traces/sra/) under the reference PRJNA213050. The reference transcriptome is publicly available from the transcriptomic database of *Biomphalaria glabrata* at the IHPE website (http://ihpe.univ-perp.fr/acces-aux-donnees/)

Competing interests

The authors declare that they have no competing interests.

Funding

This work was supported by the French National Agency for Research (ANR) through the Invimory project grant [ANR-13-JSV7-0009] to BG. The funding agency had no role in study design, collection, analysis or interpretation of data and in writing of the manuscript.

Authors' contributions

Conceived and designed the experiments: AP, SP, RG, DD, BG. Performed the experiments: AP, SP, CC, GMC, JFA. Analysed the data: AP, SP, CC, RG, GMC, DD, BG. AP, RG, BG led the manuscript writing. All authors participated in manuscript writing, editing and critical reviewing. All authors read and approved the final manuscript.

Authors' information

SP current position Welcome Trust Sanger Institute, CB10 1SA Hinxton, United Kingdom

References:

1. WHO. 2010. Schistosomiasis *Fact Sheet No. 115. World Health Organisation.*
2. Basch, P. F. 1976. Intermediate host specificity in Schistosoma mansoni. *Experimental parasitology* 39:150-169.
3. Mitta, G., C. M. Adema, B. Gourbal, E. S. Loker, and A. Theron. 2012. Compatibility polymorphism in snail/schistosome interactions: From field to theory to molecular mechanisms. *Developmental and comparative immunology* 37:1-8.
4. Theron, A., J. R. Pages, and A. Rognon. 1997. Schistosoma mansoni: distribution patterns of miracidia among Biomphalaria glabrata snail as related to host susceptibility and sporocyst regulatory processes. *Experimental parasitology* 85:1-9.
5. Theron, A., A. Rognon, B. Gourbal, and G. Mitta. 2014. Multi-parasite host susceptibility and multi-host parasite infectivity: a new approach of the Biomphalaria glabrata/Schistosoma mansoni compatibility polymorphism. *Infection Genetics and Evolution* 26:80-88.
6. Galinier, R., E. Roger, Y. Mone, D. Duval, A. Portet, S. Pinaud, C. Chaparro, C. Grunau, C. Genthon, E. Dubois, A. Rognon, N. Arancibia, B. Dejean, A. Theron, B. Gourbal, and G. Mitta. 2017. A multistrain approach to studying the mechanisms underlying compatibility in the interaction between Biomphalaria glabrata and Schistosoma mansoni. *PLoS neglected tropical diseases* 11:e0005398.
7. Mitta, G., B. Gourbal, C. Grunau, M. Knight, J. M. Bridger, and A. Theron. 2017. The Compatibility Between Biomphalaria glabrata Snails and Schistosoma mansoni: An Increasingly Complex Puzzle. *Adv Parasitol* 97:111-145.
8. Bonner, K. M., C. J. Bayne, M. K. Larson, and M. S. Blouin. 2012. Effects of Cu/Zn superoxide dismutase (sod1) genotype and genetic background on growth, reproduction and defense in Biomphalaria glabrata. *PLoS neglected tropical diseases* 6:e1701.
9. Goodall, C. P., R. C. Bender, J. K. Brooks, and C. J. Bayne. 2006. Biomphalaria glabrata cytosolic copper/zinc superoxide dismutase (SOD1) gene: association of SOD1 alleles with resistance/susceptibility to Schistosoma mansoni. *Molecular and biochemical parasitology* 147:207-210.
10. Tennessen, J. A., A. Theron, M. Marine, J. Y. Yeh, A. Rognon, and M. S. Blouin. 2015. Hyperdiverse gene cluster in snail host conveys resistance to human schistosome parasites. *PLoS genetics* 11:e1005067.
11. Ittiprasert, W., A. Miller, J. Myers, V. Nene, N. M. El-Sayed, and M. Knight. 2010. Identification of immediate response genes dominantly expressed in juvenile resistant and susceptible Biomphalaria glabrata snails upon exposure to Schistosoma mansoni. *Molecular and biochemical parasitology* 169:27-39.
12. Lockyer, A. E., A. M. Emery, R. A. Kane, A. J. Walker, C. D. Mayer, G. Mitta, C. Coustau, C. M. Adema, B. Hanelt, D. Rollinson, L. R. Noble, and C. S. Jones. 2012. Early differential gene expression in haemocytes from resistant and susceptible Biomphalaria glabrata strains in response to Schistosoma mansoni. *PLoS One* 7:e51102.
13. Lockyer, A. E., L. R. Noble, D. Rollinson, and C. S. Jones. 2004. Schistosoma mansoni: resistant specific infection-induced gene expression in Biomphalaria glabrata identified by fluorescent-based differential display. *Experimental parasitology* 107:97-104.

14. Lockyer, A. E., J. N. Spinks, A. J. Walker, R. A. Kane, L. R. Noble, D. Rollinson, E. Dias-Neto, and C. S. Jones. 2007. Biomphalaria glabrata transcriptome: identification of cell-signalling, transcriptional control and immune-related genes from open reading frame expressed sequence tags (ORESTES). *Developmental and comparative immunology* 31:763-782.
15. Roger, E., C. Grunau, R. J. Pierce, H. Hirai, B. Gourbal, R. Galinier, R. Emans, I. M. Cesari, C. Cosseau, and G. Mitta. 2008. Controlled Chaos of Polymorphic Mucins in a Metazoan Parasite (Schistosoma mansoni) Interacting with Its Invertebrate Host (Biomphalaria glabrata). *PLoS neglected tropical diseases* 2:e330.
16. Bender, R. C., C. P. Goodall, M. S. Blouin, and C. J. Bayne. 2007. Variation in expression of Biomphalaria glabrata SOD1: a potential controlling factor in susceptibility/resistance to Schistosoma mansoni. *Developmental and comparative immunology* 31:874-878.
17. Galinier, R., J. Portela, Y. Mone, J. F. Allienne, H. Henri, S. Delbecq, G. Mitta, B. Gourbal, and D. Duval. 2013. Biomphalysin, a new beta pore-forming toxin involved in Biomphalaria glabrata immune defense against Schistosoma mansoni. *PLoS pathogens* 9:e1003216.
18. Hahn, U. K., R. C. Bender, and C. J. Bayne. 2001. Involvement of nitric oxide in killing of Schistosoma mansoni sporocysts by hemocytes from resistant Biomphalaria glabrata. *Journal of Parasitology* 87:778-785.
19. Larson, M. K., R. C. Bender, and C. J. Bayne. 2014. Resistance of Biomphalaria glabrata 13-16-R1 snails to Schistosoma mansoni PR1 is a function of haemocyte abundance and constitutive levels of specific transcripts in haemocytes. *International journal for parasitology* 44:343-353.
20. Mone, Y., B. Gourbal, D. Duval, L. Du Pasquier, S. Kieffer-Jaquinod, and G. Mitta. 2010. A large repertoire of parasite epitopes matched by a large repertoire of host immune receptors in an invertebrate host/parasite model. *PLoS neglected tropical diseases* 4.
21. Myers, J., W. Ittiprasert, N. Raghavan, A. Miller, and M. Knight. 2008. Differences in cysteine protease activity in Schistosoma mansoni-resistant and -susceptible Biomphalaria glabrata and characterization of the hepatopancreas cathepsin B Full-length cDNA. *Journal of Parasitology* 94:659-668.
22. Pila, E. A., M. A. Gordy, V. K. Phillips, A. L. Kabore, S. P. Rudko, and P. C. Hanington. 2016. Endogenous growth factor stimulation of hemocyte proliferation induces resistance to Schistosoma mansoni challenge in the snail host. *Proceedings of the National Academy of Sciences of the United States of America* 113:5305-5310.
23. Roger, E., G. Mitta, Y. Mone, A. Bouchut, A. Rognon, C. Grunau, J. Boissier, A. Theron, and B. E. Gourbal. 2008. Molecular determinants of compatibility polymorphism in the Biomphalaria glabrata/Schistosoma mansoni model: New candidates identified by a global comparative proteomics approach. *Molecular and biochemical parasitology* 157:205-216.
24. Bridger, J. M., H. D. Arican-Gotkas, H. A. Foster, L. S. Godwin, A. Harvey, I. R. Kill, M. Knight, I. S. Mehta, and M. H. Ahmed. 2014. The non-random repositioning of whole chromosomes and individual gene loci in interphase nuclei and its relevance in disease, infection, aging, and cancer. *Advances in experimental medicine and biology* 773:263-279.

25. Ittiprasert, W., and M. Knight. 2012. Reversing the resistance phenotype of the Biomphalaria glabrata snail host Schistosoma mansoni infection by temperature modulation. *PLoS pathogens* 8:e1002677.
26. Ittiprasert, W., R. Nene, A. Miller, N. Raghavan, F. Lewis, J. Hodgson, and M. Knight. 2009. Schistosoma mansoni infection of juvenile Biomphalaria glabrata induces a differential stress response between resistant and susceptible snails. *Experimental parasitology* 123:203-211.
27. Knight, M., O. Elhelu, M. Smith, B. Haugen, A. Miller, N. Raghavan, C. Wellman, C. Cousin, F. Dixon, V. Mann, G. Rinaldi, W. Ittiprasert, and P. J. Brindley. 2015. Susceptibility of Snails to Infection with Schistosomes is influenced by Temperature and Expression of Heat Shock Proteins. *Epidemiology* 5:pii: 189. Epub.
28. Nelson, M. K., B. C. Cruz, K. L. Buena, H. Nguyen, and J. T. Sullivan. 2016. Effects of abnormal temperature and starvation on the internal defense system of the schistosome-transmitting snail Biomphalaria glabrata. *Journal of invertebrate pathology*.
29. Perrin, C., J. M. Lepesant, E. Roger, D. Duval, S. Fneich, V. Thuillier, J. F. Alliene, G. Mitta, C. Grunau, and C. Cosseau. 2012. Schistosoma mansoni mucin gene (SmPoMuc) expression: epigenetic control to shape adaptation to a new host. *PLoS pathogens* 9:e1003571.
30. Portet, A., S. Pinaud, G. Tetreau, R. Galinier, C. Cosseau, D. Duval, C. Grunau, G. Mitta, and B. Gourbal. 2017. Integrated multi-omic analyses in Biomphalaria-Schistosoma dialogue reveal the immunobiological significance of FREP-SmPoMuc interaction. *Developmental and comparative immunology* doi: 10.1016/j.dci.2017.02.025.
31. Osnas, E. E., P. J. Hurtado, and A. P. Dobson. 2015. Evolution of pathogen virulence across space during an epidemic. *The American naturalist* 185:332-342.
32. Tack, A. J., P. H. Thrall, L. G. Barrett, J. J. Burdon, and A. L. Laine. 2012. Variation in infectivity and aggressiveness in space and time in wild host-pathogen systems: causes and consequences. *Journal of evolutionary biology* 25:1918-1936.
33. Prugnolle, F., T. de Meeus, J. P. Pointier, P. Durand, A. Rognon, and A. Theron. 2006. Geographical variations in infectivity and susceptibility in the host-parasite system Schistosoma mansoni/Biomphalaria glabrata: no evidence for local adaptation. *Parasitology* 133:313-319.
34. Richards, C. S. 1975. Genetic factors in susceptibility of Biomphalaria glabrata for different strains of Schistosoma mansoni. *Parasitology* 70:231-241.
35. Frank, S. A. 1996. Models of parasite virulence. *The Quarterly review of biology* 71:37-78.
36. Kawecki, T., and D. Ebert. 2004. Conceptual issues in local adaptation. *Ecology letters* 7:1225-1241.
37. Kalbe, M., C. Eizaguirre, J. P. Scharsack, and P. J. Jakobsen. 2016. Reciprocal cross infection of sticklebacks with the diphyllobothriidean cestode Schistocephalus solidus reveals consistent population differences in parasite growth and host resistance. *Parasites & vectors* 9:130.
38. Ebert, D. 1994. Virulence and local adaptation of horizontally transmitted parasite. *Science* 265:1084-1086.
39. Lively, C. M. 1989. Adaptation by a Parasitic Trematode to Local Populations of Its Snail Host. *Evolution; international journal of organic evolution* 43(8).

862 40. Morand, S., S. D. Manning, and M. E. Woolhouse. 1996. Parasite-host coevolution
863 and geographic patterns of parasite infectivity and host susceptibility. *Proceedings of*
864 *the Royal Society B* 263:119-128.
865 41. Osnas, E. E., and C. M. Lively. 2004. Parasite dose, prevalence of infection and local
866 adaptation in a host-parasite system. *Parasitology* 128:223-228.
867 42. Mone, Y., A. C. Ribou, C. Cosseau, D. Duval, A. Theron, G. Mitta, and B. Gourbal. 2011.
868 An example of molecular co-evolution: reactive oxygen species (ROS) and ROS
869 scavenger levels in Schistosoma mansoni/Biomphalaria glabrata interactions.
870 *International journal for parasitology* 41:721-730.
871 43. Penczykowski, R. M., A. L. Laine, and B. Koskella. 2015. Understanding the ecology
872 and evolution of host-parasite interactions across scales. *Evolutionary applications*
873 9:37-52.
874 44. Robertson, S., J. E. Bradley, and A. D. MacColl. 2017. No evidence of local adaptation
875 of immune responses to Gyrodactylus in three-spined stickleback (Gasterosteus
876 aculeatus). *Fish and Shellfish Immunology* 60:275-281.
877 45. Bankers, L., P. Fields, K. E. McElroy, J. L. Boore, J. M. Logsdon, Jr., and M. Neiman.
878 2018. Genomic evidence for population-specific responses to co-evolving parasites in
879 a New Zealand freshwater snail. *Mol Ecol* 26:3663-3675.
880 46. Kincaid-Smith, J., O. Rey, E. Toulza, A. Berry, and J. Boissier. 2017. Emerging
881 Schistosomiasis in Europe: A Need to Quantify the Risks. *Trends in Parasitology*
882 33:600-609.
883 47. Dheilly, N. M., D. Duval, G. Mouahid, R. Emans, J. F. Allienne, R. Galinier, C. Genthon,
884 E. Dubois, L. Du Pasquier, C. M. Adema, C. Grunau, G. Mitta, and B. Gourbal. 2015. A
885 family of variable immunoglobulin and lectin domain containing molecules in the
886 snail Biomphalaria glabrata. *Developmental and comparative immunology* 48:234-
887 243.
888 48. Pinaud, S., J. Portela, D. Duval, F. C. Nowacki, M. A. Olive, J. F. Allienne, R. Galinier, N.
889 M. Dheilly, S. Kieffer-Jaquinod, G. Mitta, A. Theron, and B. Gourbal. 2016. A Shift
890 from Cellular to Humoral Responses Contributes to Innate Immune Memory in the
891 Vector Snail Biomphalaria glabrata. *PLoS pathogens* 12:e1005361.
892 49. Sminia, T., and L. Barendsen. 1980. A comparative morphological and enzyme
893 histochemical study on blood cells of the freshwater snails, *Lymnaea stagnalis*,
894 *Biomphalaria glabrata*, and *Bulinus truncatus*. *Journal of Morphology* 165:31-39.
895 50. Zhao, X., H. Yu, L. Kong, S. Liu, and Q. Li. 2016. High throughput sequencing of small
896 RNAs transcriptomes in two Crassostrea oysters identifies microRNAs involved in
897 osmotic stress response. *Scientific reports* 6:22687.
898 51. Enright, A. J., B. John, U. Gaul, T. Tuschl, C. Sander, and D. S. Marks. 2003. MicroRNA
899 targets in Drosophila. *Genome Biology* 5:R1.
900 52. Baeza Garcia, A., R. J. Pierce, B. Gourbal, E. Werkmeister, D. Colinet, J. M. Reichhart,
901 C. Dissous, and C. Coustau. 2010. Involvement of the cytokine MIF in the snail host
902 immune response to the parasite Schistosoma mansoni. *PLoS pathogens* 6:e1001115.
903 53. Guillou, F., E. Roger, Y. Mone, A. Rognon, C. Grunau, A. Theron, G. Mitta, C. Coustau,
904 and B. E. Gourbal. 2007. Excretory-secretory proteome of larval Schistosoma
905 mansoni and Echinostoma caproni, two parasites of Biomphalaria glabrata. *Molecular*
906 *and biochemical parasitology*.
907 54. Raghavan, M., S. J. Wijeyesakere, L. R. Peters, and N. Del Cid. 2013. Calreticulin in the
908 immune system: ins and outs. *Trends in Immunology* 34:13-21.

909 55. Ryu, S. J., and S. C. Park. 2009. Targeting major vault protein in senescence-
910 associated apoptosis resistance. *Expert Opinion on Therapeutic Targets* 13:479-484.
911 56. Gilges, D., M. A. Vinit, I. Callebaut, L. Coulombel, V. Cacheux, P. H. Romeo, and I.
912 Vigon. 2000. Polydom: a secreted protein with pentraxin, complement control
913 protein, epidermal growth factor and von Willebrand factor A domains. *Biochemical*
914 *Journal* 352 Pt 1:49-59.
915 57. Bohdanowicz, M., D. Schlam, M. Hermansson, D. Rizzuti, G. D. Fairn, T. Ueyama, P.
916 Somerharju, G. Du, and S. Grinstein. 2013. Phosphatidic acid is required for the
917 constitutive ruffling and macropinocytosis of phagocytes. *Molecular Biology of the*
918 *Cell* 24:1700-1712, S1701-1707.
919 58. Grkovich, A., and E. A. Dennis. 2009. Phosphatidic acid phosphohydrolase in the
920 regulation of inflammatory signaling. *Advances in Enzyme Regulation* 49:114-120.
921 59. Dybdahl, M. F., and A. Storfer. 2003. Parasite local adaptation: Red Queen versus
922 suicide king. *TRENDs in Ecology and Evolution* 18:523-530.
923 60. Osnas, E. E., and C. M. Lively. 2005. Immune response to sympatric and allopatric
924 parasites in a snail-trematode interaction. *Frontiers in Zoology* 2:8.
925 61. Ebert, D. 1998. Experimental evolution of parasites. *Science* 282:1432-1435.
926 62. Minchella, D. J. 1985. Host life-history variation in response to parasitism.
927 *Parasitology* 90:205-216.
928 63. Greischar, M. A., and B. Koskella. 2007. A synthesis of experimental work on parasite
929 local adaptation. *Ecology letters* 10:418-434.
930 64. Adema, C. M., L. A. Hertel, R. D. Miller, and E. S. Loker. 1997. A family of fibrinogen-
931 related proteins that precipitates parasite-derived molecules is produced by an
932 invertebrate after infection. *Proceedings of the National Academy of Sciences of the*
933 *United States of America* 94:8691-8696.
934 65. Zhang, H., L. Song, C. Li, J. Zhao, H. Wang, Q. Gao, and W. Xu. 2007. Molecular cloning
935 and characterization of a thioester-containing protein from Zhikong scallop Chlamys
936 farreri. *Molecular Immunology* 44:3492-3500.
937 66. Cavalcanti, M. G., F. C. Filho, A. M. Mendonca, G. R. Duarte, C. C. Barbosa, C. M. De
938 Castro, L. C. Alves, and F. A. Brayner. 2012. Morphological characterization of
939 hemocytes from Biomphalaria glabrata and Biomphalaria straminea. *Micron* 43:285-
940 291.
941 67. Li, S., L. Shen, L. Sun, J. Xu, P. Jin, L. Chen, and F. Ma. 2017. Small RNA-Seq analysis
942 reveals microRNA-regulation of the Imd pathway during Escherichia coli infection in
943 Drosophila. *Developmental and comparative immunology* 70:80-87.
944 68. Zawada, A. M., L. Zhang, I. E. Emrich, K. S. Rogacev, N. Krezdorn, B. Rotter, D. Fliser, Y.
945 Devaux, L. Ziegler-Heitbrock, and G. H. Heine. 2017. MicroRNA profiling of human
946 intermediate monocytes. *Immunobiology* 222:587-596.
947 69. Meningher, T., G. Lerman, N. Regev-Rudzki, D. Gold, I. Z. Ben-Dov, Y. Sidi, D. Avni, and
948 E. Schwartz. 2017. Schistosomal MicroRNAs Isolated From Extracellular Vesicles in
949 Sera of Infected Patients: A New Tool for Diagnosis and Follow-up of Human
950 Schistosomiasis. *Journal of Infectious Diseases* 215:378-386.
951 70. Nowacki, F. C., M. T. Swain, O. I. Klychnikov, U. Niazi, A. Ivens, J. F. Quintana, P. J.
952 Hensbergen, C. H. Hokke, A. H. Buck, and K. F. Hoffmann. 2015. Protein and small
953 non-coding RNA-enriched extracellular vesicles are released by the pathogenic blood
954 fluke Schistosoma mansoni. *Journal of Extracellular Vesicles* 4:28665.

955 71. Walzer, K. A., and J. T. Chi. 2017. Trans-kingdom small RNA transfer during host-
956 pathogen interactions: The case of P. falciparum and erythrocytes. *RNA Biology*:1-8.
957 72. Hanington, P. C., M. A. Forys, and E. S. Loker. 2012. A somatically diversified defense
958 factor, FREP3, is a determinant of snail resistance to schistosome infection. *PLoS*
959 *neglected tropical diseases* 6:e1591.
960 73. Jiang, Y., E. S. Loker, and S. M. Zhang. 2006. In vivo and in vitro knockdown of FREP2
961 gene expression in the snail Biomphalaria glabrata using RNA interference.
962 *Developmental and comparative immunology* 30:855-866.
963 74. Tetreau, G., S. Pinaud, A. Portet, R. Galinier, B. Gourbal, and D. Duval. 2017. Specific
964 Pathogen Recognition by Multiple Innate Immune Sensors in an Invertebrate. *Front*
965 *Immunol* 8:1249.
966 75. Van Der Knaap, W. P. W., and E. S. Loker. 1990. Immune mechanisms in trematod-
967 snail interactions. *Parasitology Today* 6:175-182.
968 76. Crellen, T., F. Allan, S. David, C. Durrant, T. Huckvale, N. Holroyd, A. M. Emery, D.
969 Rollinson, D. M. Aanensen, M. Berriman, J. P. Webster, and J. A. Cotton. 2016. Whole
970 genome resequencing of the human parasite Schistosoma mansoni reveals
971 population history and effects of selection. *Scientific reports* 6:20954.
972 77. Lockyer, A. E., P. D. Olson, P. Ostergaard, D. Rollinson, D. A. Johnston, S. W. Attwood,
973 V. R. Southgate, P. Horak, S. D. Snyder, T. H. Le, T. Agatsuma, D. P. McManus, A. C.
974 Carmichael, S. Naem, and D. T. Littlewood. 2003. The phylogeny of the
975 Schistosomatidae based on three genes with emphasis on the interrelationships of
976 Schistosoma Weinland, 1858. *Parasitology* 126:203-224.
977 78. Morgan, J. A., R. J. Dejong, G. O. Adeoye, E. D. Ansa, C. S. Barbosa, P. Bremond, I. M.
978 Cesari, N. Charbonnel, L. R. Correa, G. Coulibaly, P. S. D'Andrea, C. P. De Souza, M. J.
979 Doenhoff, S. File, M. A. Idris, R. N. Incani, P. Jarne, D. M. Karanja, F. Kazibwe, J. Kpikpi,
980 N. J. Lwambo, A. Mabaye, L. A. Magalhaes, A. Makundi, H. Mone, G. Mouahid, G. M.
981 Muchemi, B. N. Mungai, M. Sene, V. Southgate, L. A. Tchuente, A. Theron, F. Yousif,
982 E. M. Zanotti-Magalhaes, G. M. Mkoji, and E. S. Loker. 2005. Origin and diversification
983 of the human parasite Schistosoma mansoni. *Molecular ecology* 14:3889-3902.
984 79. Campbell, G., C. S. Jones, A. E. Lockyer, S. Hughes, D. Brown, L. R. Noble, and D.
985 Rollinson. 2000. Molecular evidence supports an african affinity of the neotropical
986 freshwater gastropod, Biomphalaria glabrata, say 1818, an intermediate host for
987 Schistosoma mansoni. *Proceedings of the Royal Society B* 267:2351-2358.
988 80. DeJong, R. J., J. A. Morgan, W. L. Paraense, J. P. Pointier, M. Amarista, P. F. Ayeh-
989 Kumi, A. Babiker, C. S. Barbosa, P. Bremond, A. Pedro Canese, C. P. de Souza, C.
990 Dominguez, S. File, A. Gutierrez, R. N. Incani, T. Kawano, F. Kazibwe, J. Kpikpi, N. J.
991 Lwambo, R. Mimpfoundi, F. Njiokou, J. Noel Poda, M. Sene, L. E. Velasquez, M. Yong,
992 C. M. Adema, B. V. Hofkin, G. M. Mkoji, and E. S. Loker. 2001. Evolutionary
993 relationships and biogeography of Biomphalaria (Gastropoda: Planorbidae) with
994 implications regarding its role as host of the human bloodfluke, Schistosoma
995 mansoni. *Molecular biology and evolution* 18:2225-2239.
996 81. Theron, A. 2005. Les schistosomes et leurs hôtes : apport des marqueurs
997 moléculaires à la connaissance de leur phylogéographie, épidémiologie et écologie.
998 *Bulletin de la Société Zoologique de France* 130 205-218.
999 82. Morgan, J. A., R. J. Dejong, S. D. Snyder, G. M. Mkoji, and E. S. Loker. 2001.
1000 Schistosoma mansoni and Biomphalaria: past history and future trends. *Parasitology*
1001 123 Suppl:S211-228.

1002 83. Boissier, J., S. Grech-Angelini, B. L. Webster, J. F. Allienne, T. Huyse, S. Mas-Coma, E.
1003 Toulza, H. Barre-Cardi, D. Rollinson, J. Kincaid-Smith, A. Oleaga, R. Galinier, J. Foata,
1004 A. Rognon, A. Berry, G. Mouahid, R. Henneron, H. Mone, H. Noel, and G. Mitta. 2016.
1005 Outbreak of urogenital schistosomiasis in Corsica (France): an epidemiological case
1006 study. *The Lancet Infectious Diseases* 16:971-979.
1007 84. Boissier, J., H. Mone, G. Mitta, M. D. Bargues, D. Molyneux, and S. Mas-Coma. 2015.
1008 Schistosomiasis reaches Europe. *The Lancet Infectious Diseases* 15:757-758.
1009
1010
1011

Figure Legends

FIGURE 1. Dual-RNAseq of Biomphalaria immune-related transcripts. Among the differentially represented transcripts, Blast2GO functional annotation allowed us to identify 336 transcripts that appeared to be related to the *Biomphalaria* immune response. Abbreviations and colours: blue BB, sympatric interaction between BgBRE and SmBRE; green BV, allopatric interaction between BgBRE and SmVEN; and red BR, allopatric interaction between BgBRE and Srod. For each interaction 40 whole-snails are used, 20 pooled at 24 h and 20 at 96 h post-infection. A) Venn diagram showing the relationships among the immune transcripts found to be differentially expressed in the sympatric and allopatric interactions. B) Clustering of differentially represented immune transcripts. Heatmap representing the profiles of the 336 differentially represented immune-related transcripts in the BB, BV or BR interactions along the kinetic of infection (at 24 and 96 h). Each transcript is represented once, and each line represents one transcript. Colours: yellow, overrepresented transcripts; purple, underrepresented transcripts; and black, unchanged relative to levels in control naïve snails. C) Pie chart showing the distribution of the selected immune-related transcripts across three immunological processes: immune recognition (pink), immune effectors (brown) and immune signalling (blue). For each category and interaction, the respective proportion of transcripts and the direction of the effect (over- or under-expression) are indicated.

FIGURE 2. Differentially represented immune-related transcripts in sympatric and allopatric interactions. Cumulative expression [Log2FC (fold change) from DESeq2 analysis] of the immune-related transcripts identified as being differentially represented following sympatric or allopatric infection. Transcripts were grouped into the three immunological groups described in Fig. 1, and from there into functional categories. The yellow histograms correspond to cumulatively overrepresented transcripts, while the purple histograms show underrepresented transcripts. The black (overrepresented) and gray (underrepresented) diamonds correspond to the number of transcripts analysed in each functional category. Abbreviations: BB, BgBRE/SmBRE interaction; BV, BgBRE/SmVEN interaction; and BR, BgBRE/Srod interaction. A. Immune transcript expression at 24 h post-infection. B. Immune transcript expression at 96 h post-infection.

FIGURE 3. Microscopic analysis of snail hemocyte proliferations. In vitro EdU-labelling of hemocytes was conducted for sympatric and allopatric interactions. A) Hemocytes were collected at 24 h post-infection for in vitro analysis. Confocal microscopy of EdU-labeled hemocytes from snails subjected to the allopatric BV interaction (BgBRE/SmVEN). Colours: blue, DAPI; and green, EdU. B) Microscopic counting of EdU-labelled hemocytes from naïve control snails (BgBRE) (n = 1,811) and those subjected to the sympatric interaction (BB: BgBRE/SmBRE) (n=2,064) or an allopatric interaction (BV: BgBRE/SmVEN) (n = 1,366) recovered from three individual snails by condition. Colours: green, EdU-positive cells; and blue, EdU-negative cells. Between-group differences in the percentage of proliferation were tested using a Fisher exact test, with statistical significance accepted at $p < 0.05$. The “a” indicates a significant difference between the naïve and infective conditions, while “b” indicates a significant difference between the infective conditions.

FIGURE 4. Flow cytometry analysis of the hemocyte response in sympatric and allopatric interactions. A) Flow cytometry was used to count in vivo EdU-labelled hemocytes at 24 h and 96 h after infection in sympatric and allopatric interactions. A total number of hemocytes of n = 10,000 were recovered for six biological replicates of

three snails. Control naïve snails (BgBRE, yellow) were compared to those subjected to the sympatric interaction (BB, BgBRE/SmBRE, blue) or an allopatric interaction (BV, BgBRE/SmVEN, green). B) The experiment described in A was repeated using the BgVEN snail strain. Control naïve snails (BgVEN, yellow) were compared to those subjected to the sympatric interaction (VV, BgVEN/SmVEN, green) or an allopatric interaction (VB, BgVEN/SmBRE, blue). C) FSC (forward-scattered light, representing cell size) and SSC (side-scattered light, representing cell granularity) circulating hemocyte patterns in BgBRE snails under the naïve condition (yellow) or 24 h and 96 h after infections in sympatry (BB24/96, BgBRE/SmBRE, blue) or allopatry (BV24/96, BgBRE/SmVEN, green). D) FSC and SSC circulating hemocyte patterns in BgVEN snails under the naïve condition (yellow) or 24 h and 96 h after infections in sympatry (VV24/96, BgVEN/SmVEN, blue) or allopatry (VB24/96, BgVEN/SmBRE, green). The red dots correspond to EdU-positive hemocytes.
Between-group differences in the percentage of proliferation were tested using the Mann-Whitney U-test, with statistical significance accepted at $p < 0.05$. The "a" indicates a significant difference between the naïve and infective condition, "b" indicates a significant difference between the infective conditions at 24h, and "c" indicates a significant difference between the infective conditions at 96h.

FIGURE 5. Development of parasites into snail tissues. A histological approach was used to monitor parasite size along the course of snail infection. The sympatric interaction (BgBRE x SmBRE) is shown in blue, and the allopatric interaction (BgBRE x SmVEN) is shown in green. For each experimental interaction, the parasite sizes were quantified at 24 and 96 h after infection. Morpho-anatomical aspects of the parasite are depicted to highlight a potential difference in parasite survival. N = 7 to 10 sporocystes were used. Between-group parasite size differences were assessed using the Mann-Whitney U-test, with significance accepted at $p < 0.05$ (indicated by "a" on the histograms).

FIGURE 6. Clustering of intra-molluscalSchistosoma expression patterns. RNAseq library mapping enabled us to identify 351 genes expressed by *Schistosoma* parasites in *Biomphalaria* snail tissues. Colours: blue, *S. mansoni* Brazil (SmBRE); green, *S. mansoni* Venezuela (SmVEN); and red, *S. rodhaini* (Srod). The heatmap represents the profiles of the 351 genes expressed by the different parasites at 24 h after infection. Each transcript is represented once, and each line represents one transcript. The expression level is highlighted by the different shades of blue.

FIGURE 7. In silico identification of parasite miRNAs. miRNAs were assessed using libraries obtained from naïve snails and snails infected for 24 h under the various interaction conditions (BB24, BgBRE x SmBRE; BV24, BgBRE x SmVEN; BR24, BgBRE x Srod). A) Table highlighting the precursor miRNAs that may have targets among the immune-related snail transcripts selected in the present work. They include eight precursors specifically recovered in BB24, two in BV24, and one shared across the three infected conditions. The total numbers of potential targets in each condition are indicated. B) Venn diagram showing the potential targets according to the sympatric or allopatric interactions. Shown is an example miRNA stem-loop precursor that presents the highest number of potential host targets.

SUPPLEMENTARY FIGURE 1. Clustering of all differential represented transcripts. Clustering of differentially represented transcripts. Heatmap representing the profiles of the 1,895 differentially represented immune-related transcripts in the BB, BV or BR interactions along the time course of infection (at 24 and 96 h).

Each transcript is represented once, and each line represents one transcript. Colours: yellow, overrepresented transcripts; purple, underrepresented transcripts; and black, unchanged relative to levels in control naïve snails.

SUPPLEMENTARY FIGURE 2. Mortality of *B. glabrata* snails after infections. The survival rates of *B. glabrata* subjected to infection by different *S. mansoni* strains were observed over 14 weeks. Kaplan Meier graphs were generated using xlstat, and the log-rank test ($p < 0.05$) was used to test for significant between-group differences. Coloured curves indicate the mortality rates of naïve snails (yellow) ($n = 60$), snails infected by the sympatric parasite (BB, BgBRE/SmBRE, blue) ($n = 50$), and snails infected by the allopatric parasite (BV, BgBRE/SmVEN, green) ($n=50$). The difference in mortality between naïve and infected snails was significant ($p < 0.05$), whereas that between the two infected conditions was not ($p = 0.243$).

1109
1110
1111
1112 **TABLE 1.** Number of transcripts in each step of transcriptomic analysis

1113

Analysis of transcriptomic data		**Analyses of Blast2GO**	**Analyses of annotations**	
Full transcriptome	Differentially expressed	Informative annotation	Immune transcripts	Non-immune transcripts
159,711	3,865	1,017	336	681

1114
1115
1116
1117

SUPPLEMENTARY TABLE 1. *Biomphalaria* and *Schistosoma* compatibility between African and South American strains

			Biomphalaria		
			glabrata		*pfeifferi*
			BRE	**VEN**	**SEN**
Schistosoma mansoni	*BRE*	**P %**	**100**	70	92
		I	**3.6**	3.5	2.9
	VEN	**P %**	100	**95**	100
		I	3.2	**3.8**	4
	SEN	**P %**	27	13	**100**
		I	1.3	1	**2.5**
Schistosoma rodhaini		**P %**	80	*NA*	*NA*
		I	2	*NA*	*NA*

The prevalence (P %: percentage of snail infected) and intensity (I: number of parasites per infected host) of infection are presented for each experimental infection. The indicated values correspond to 20 miracidia. Each pairwise combination of *Biomphalaria* (BgBRE, BgVEN, BpSEN) and *Schistosomamansoni* (SmBRE, SmVEN, SmSEN) or *SchistosomaRodhaini* (Srod) were tested for compatibility. *NA*: non-available data.

Figure 1

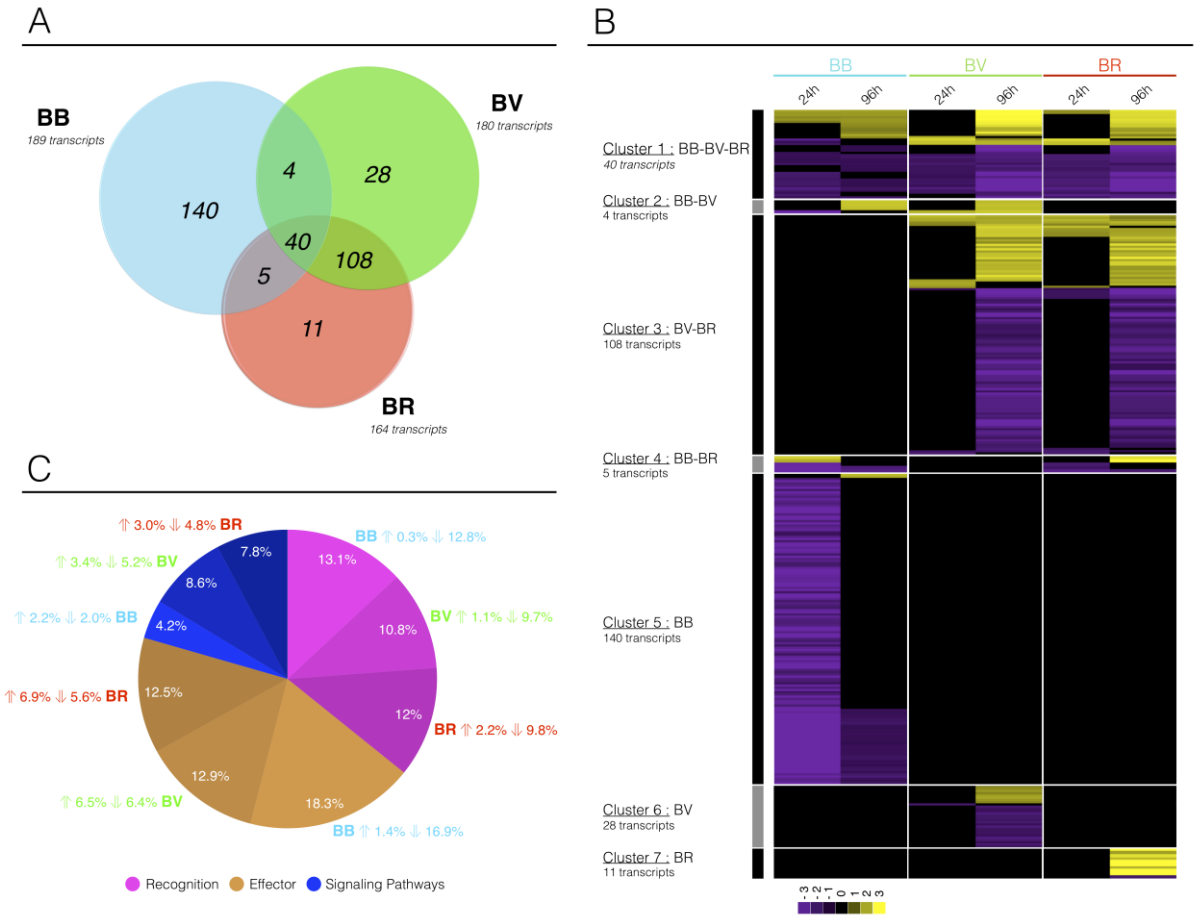
A
BB
189 transcripts
BV
180 transcripts
BR
164 transcripts
140
4
28
40
108
5
11
B
BB
BV
BR
24h
96h
Cluster 1 : BB-BV-BR
40 transcripts
Cluster 2 : BB-BV
4 transcripts
Cluster 3 : BV-BR
108 transcripts
Cluster 4 : BB-BR
5 transcripts
Cluster 5 : BB
140 transcripts
Cluster 6 : BV
28 transcripts
Cluster 7 : BR
11 transcripts
C
13.1%
BB ⇑ 0.3% ⇓ 12.8%
10.8%
BV ⇑ 1.1% ⇓ 9.7%
12%
BR ⇑ 2.2% ⇓ 9.8%
18.3%
BB ⇑ 1.4% ⇓ 16.9%
12.9%
⇑ 6.5% ⇓ 6.4% BV
12.5%
⇑ 6.9% ⇓ 5.6% BR
4.2%
⇑ 2.2% ⇓ 2.0% BB
8.6%
⇑ 3.4% ⇓ 5.2% BV
7.8%
⇑ 3.0% ⇓ 4.8% BR
Recognition
Effector
Signaling Pathways

Figure 2

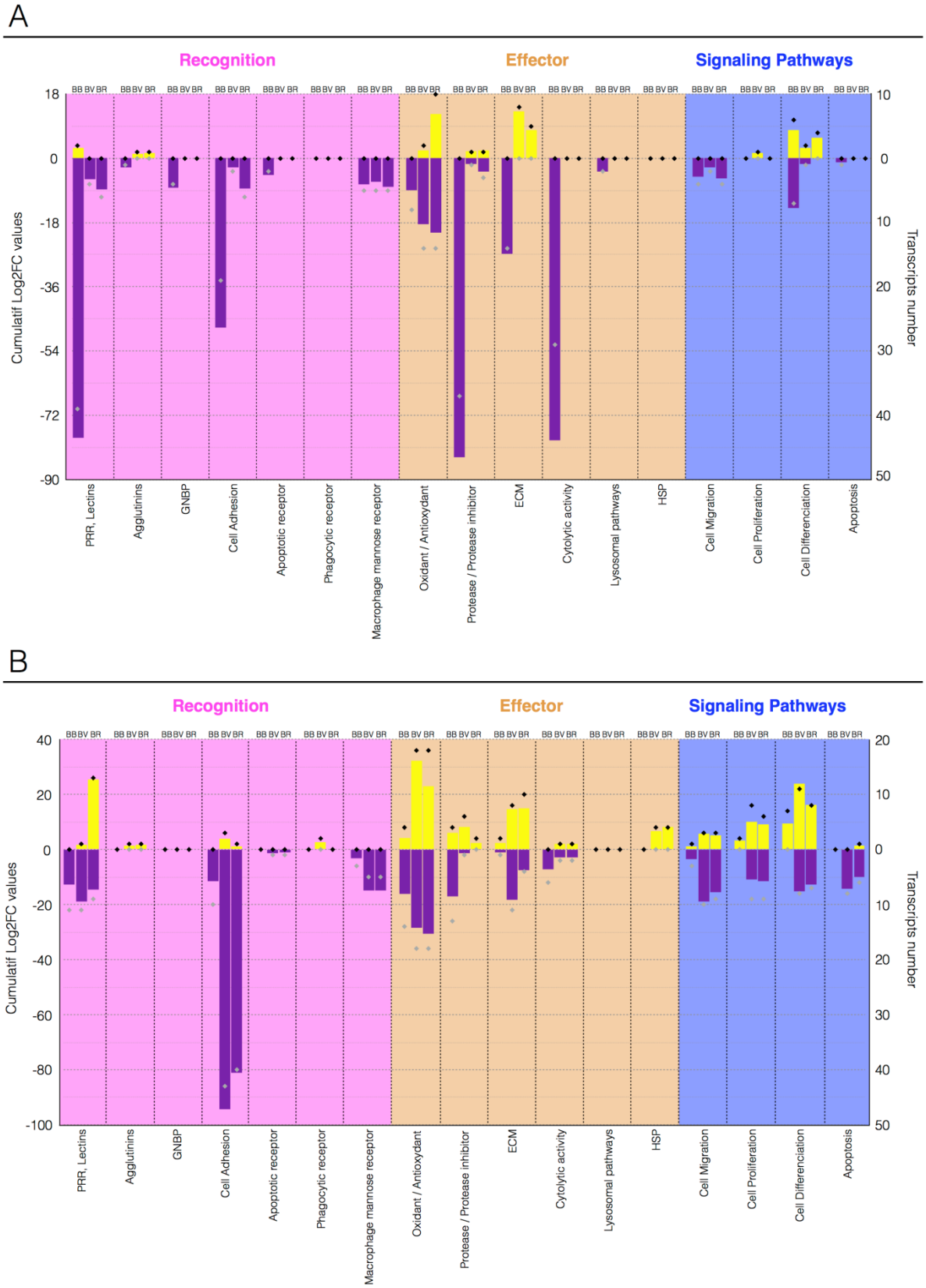
A
Recognition
Effector
Signaling Pathways
BB BV BR
Cumulatif Log2FC values
Transcripts number
PRR, Lectins
Agglutinins
GNBP
Cell Adhesion
Apoptotic receptor
Phagocytic receptor
Macrophage mannose receptor
Oxidant / Antioxydant
Protease / Protease inhibitor
ECM
Cytolytic activity
Lysosomal pathways
HSP
Cell Migration
Cell Proliferation
Cell Differenciation
Apoptosis
B
Recognition
Effector
Signaling Pathways
BB BV BR
Cumulatif Log2FC values
Transcripts number
PRR, Lectins
Agglutinins
GNBP
Cell Adhesion
Apoptotic receptor
Phagocytic receptor
Macrophage mannose receptor
Oxidant / Antioxydant
Protease / Protease inhibitor
ECM
Cytolytic activity
Lysosomal pathways
HSP
Cell Migration
Cell Proliferation
Cell Differenciation
Apoptosis

Figure 3

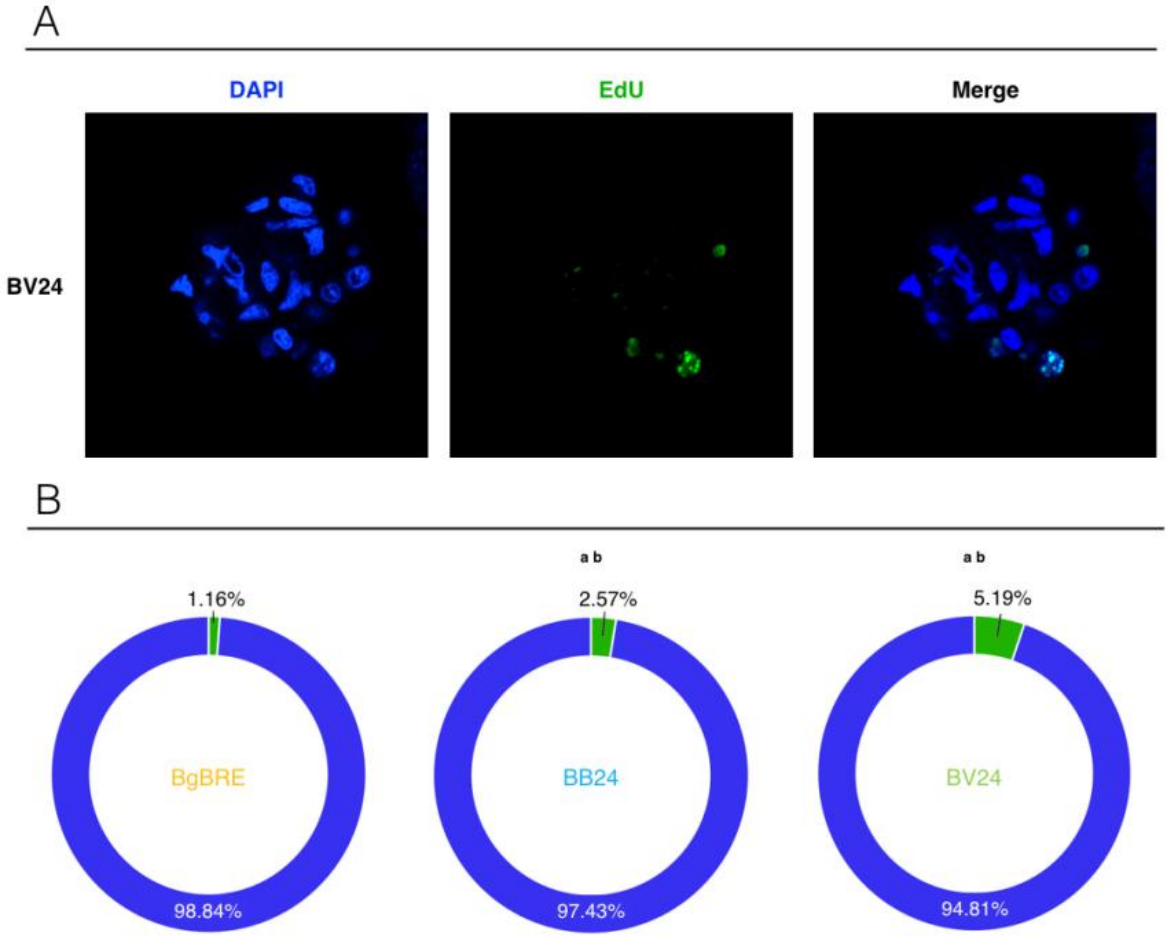
A
DAPI
EdU
Merge
BV24
B
a b
a b
1.16%
2.57%
5.19%
BgBRE
BB24
BV24
98.84%
97.43%
94.81%

Figure 4

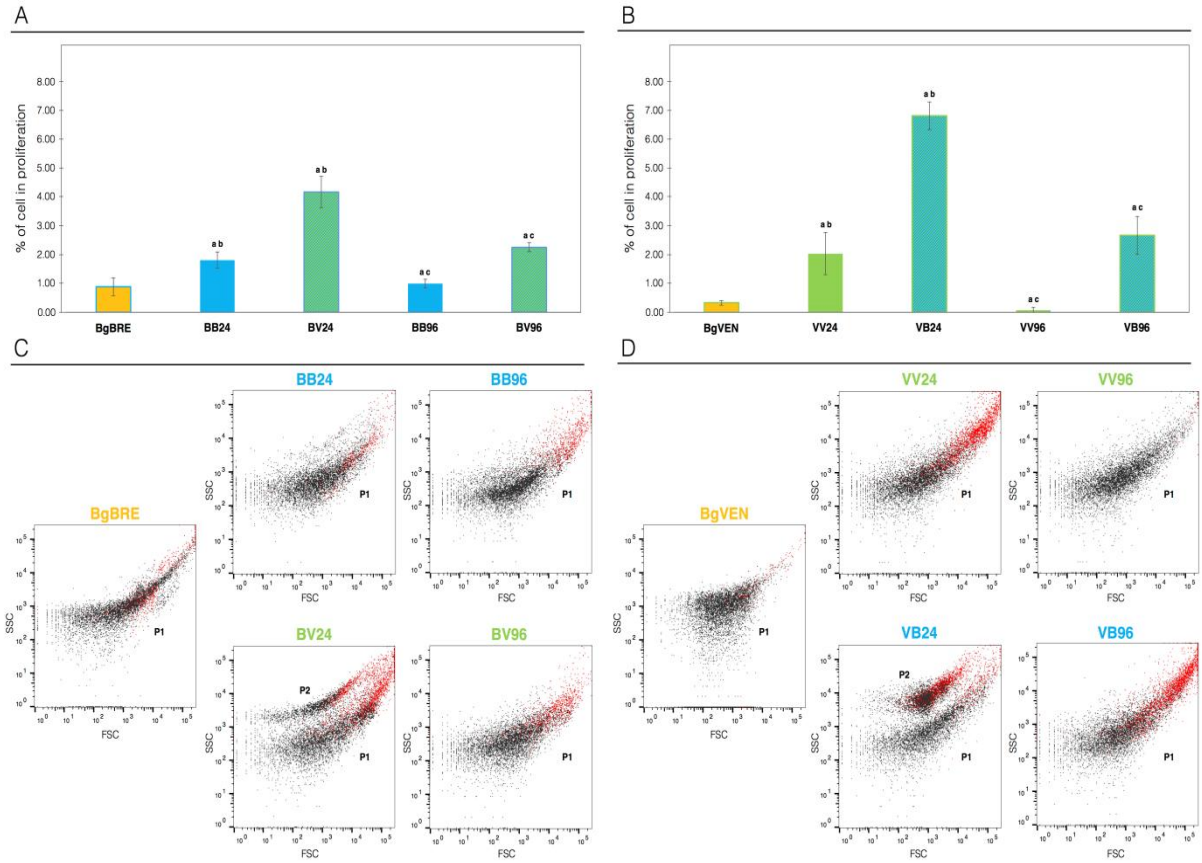
A
% of cell in proliferation
BgBRE
BB24
BV24
BB96
BV96
B
BgVEN
VV24
VB24
VV96
VB96
C
D
P1
P2
SSC
FSC

Figure 5

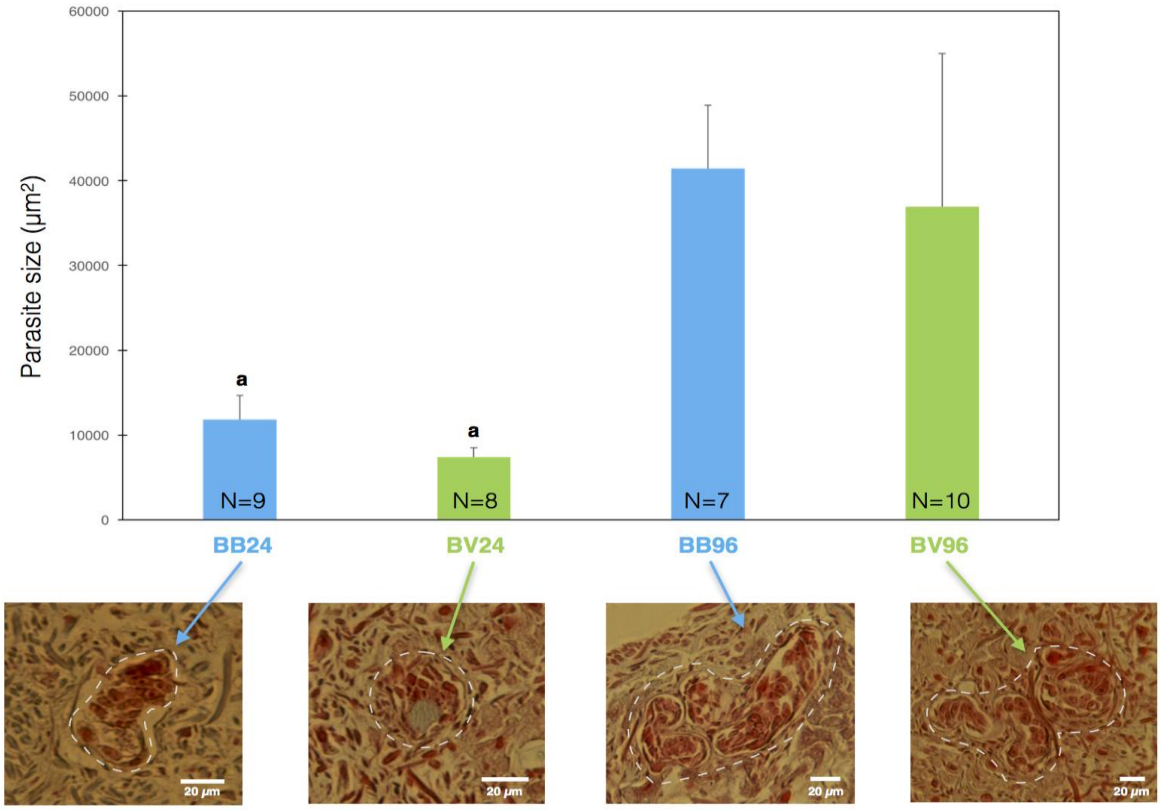
Parasite size (µm²)
60000
50000
40000
30000
20000
10000
0
a
a
N=9
N=8
N=7
N=10
BB24
BV24
BB96
BV96
20 µm
20 µm
20 µm
20 µm

Figure 6

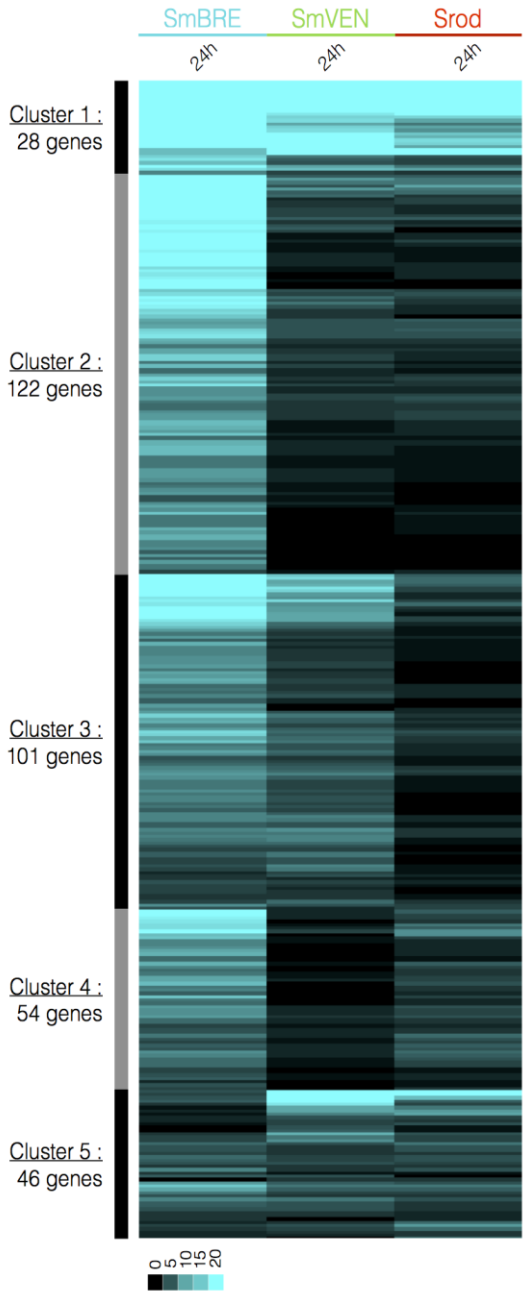
SmBRE
SmVEN
Srod
24h
24h
24h
Cluster 1 :
28 genes
Cluster 2 :
122 genes
Cluster 3 :
101 genes
Cluster 4 :
54 genes
Cluster 5 :
46 genes
0
5
10
15
20

Figure 7

A

Precursor	BgBRE duplicates		BB24	BV24	BR24	Targets
sma-mir-8460	0	0	1	0	0	7
sma-mir-8463	0	0	1	0	0	9
sma-mir-2a	0	0	1	0	0	20
sma-mir-2d	0	0	1	0	0	50
sma-mir-3492	0	0	1	0	0	10
sma-mir-8404	0	0	1	0	0	4
sma-mir-8414	0	0	1	0	0	14
sma-mir-8446	0	0	1	0	0	23
sma-mir-8456	0	0	0	1	0	2
sma-mir-8431	0	0	0	1	0	4
sma-mir-190	0	0	1	1	1	17
Sum of potential Bg targets	**0**	**0**	**154**	**23**	**17**	

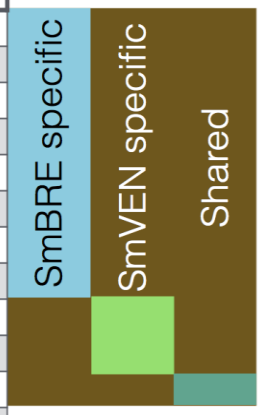

B

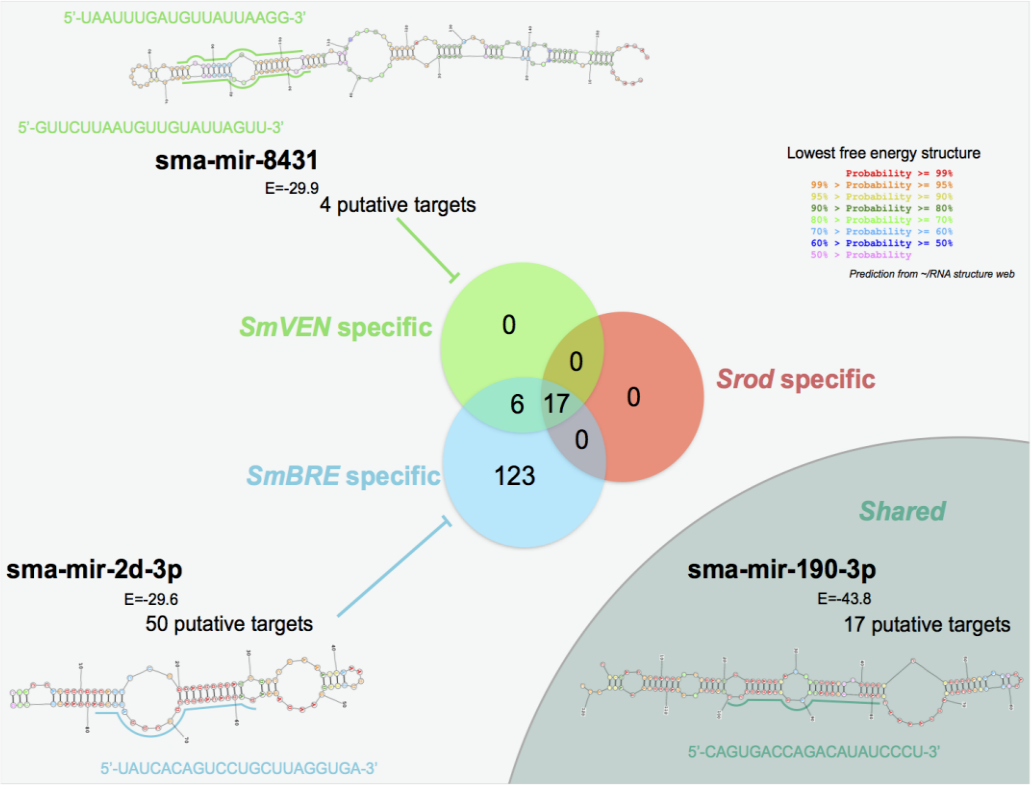

Supplementary Figure 1

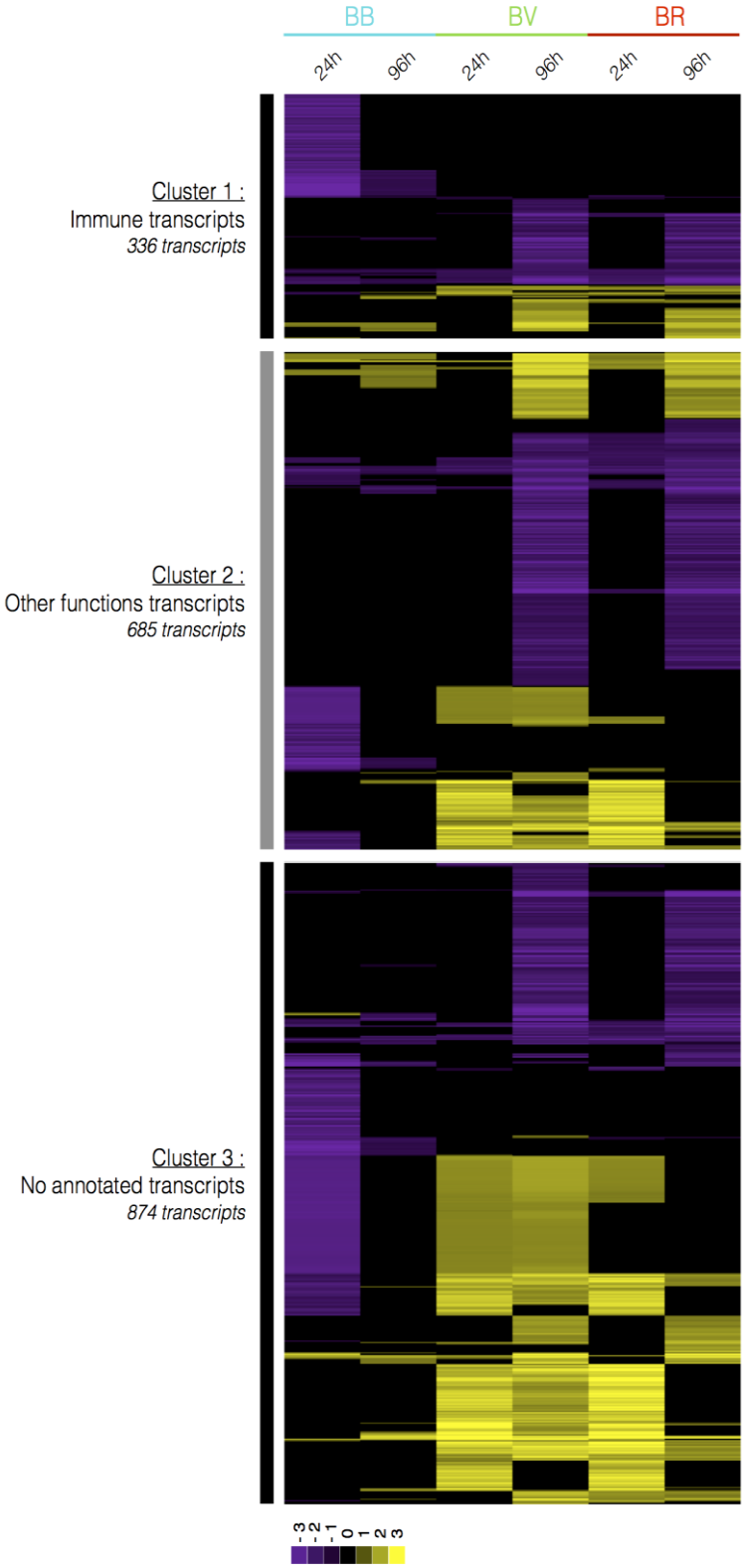
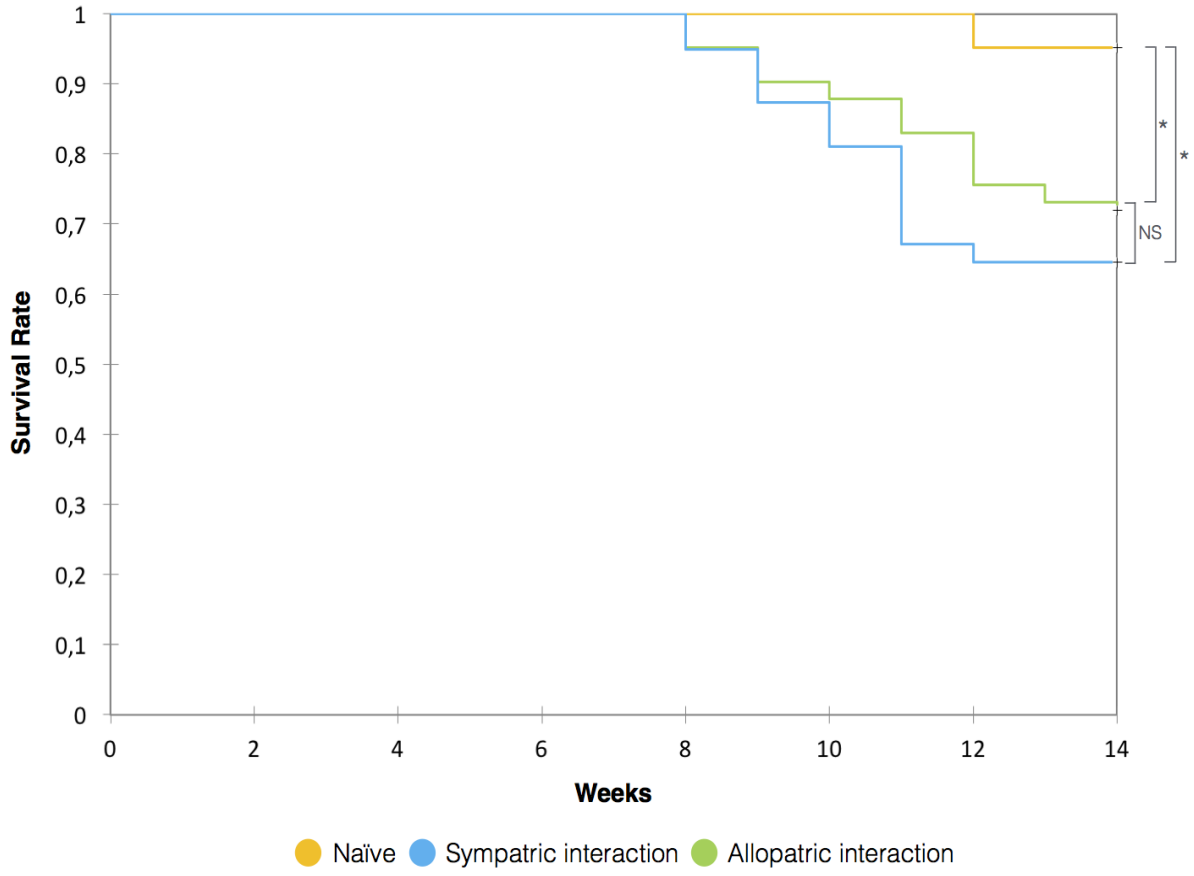
Supplementary Figure 2